



Augmented Partial Factorization: efficient computation of the generalized scattering matrix

Chia Wei (Wade) Hsu

Ming Hsieh Department of Electrical and Computer Engineering
University of Southern California

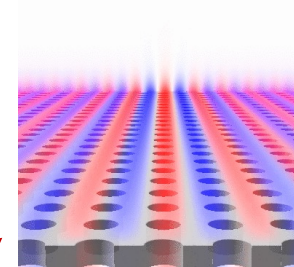
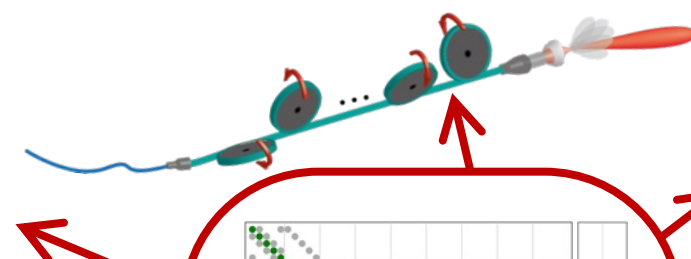
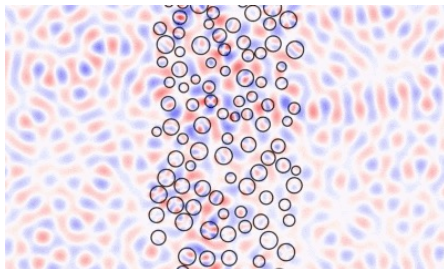
Optics in Complex Systems Group @ USC



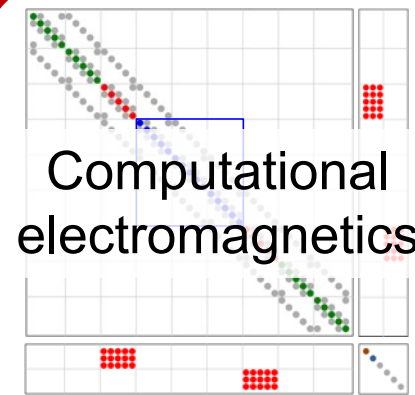
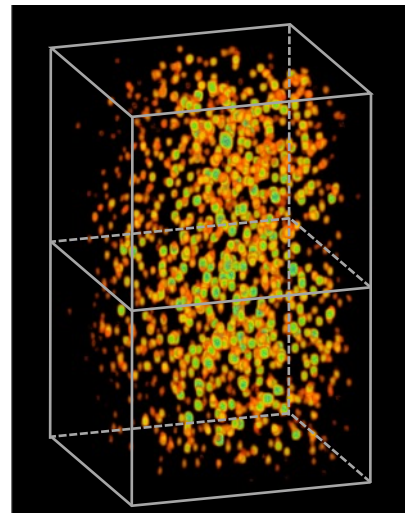
Optics in Complex Systems Group @ USC

Optical systems that couple *many degrees of freedom* (spatial/angular, temporal/spectral, etc)

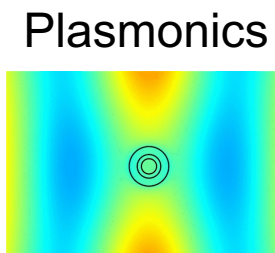
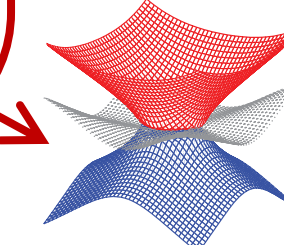
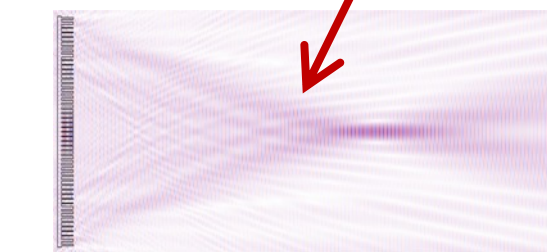
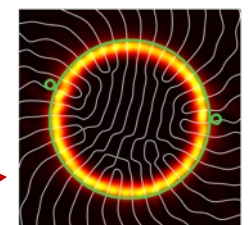
Transport through disorder & multimode fibers



Imaging in scattering media



Photonic Crystals

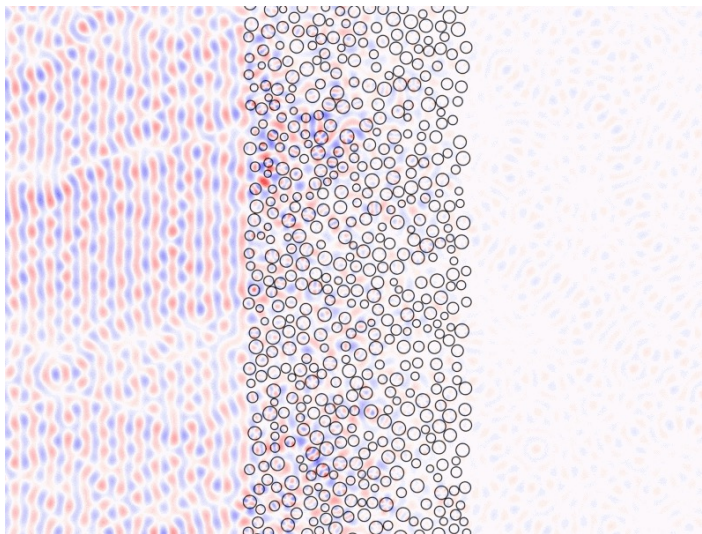


Non-Hermitian
photronics

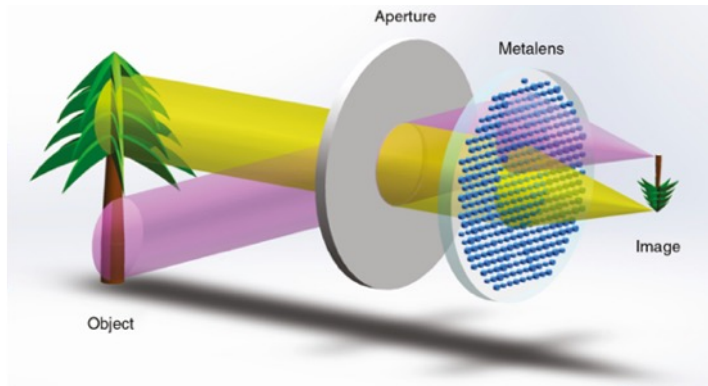
Metasurface & inverse design

Multi-channel optical systems

Disordered Media

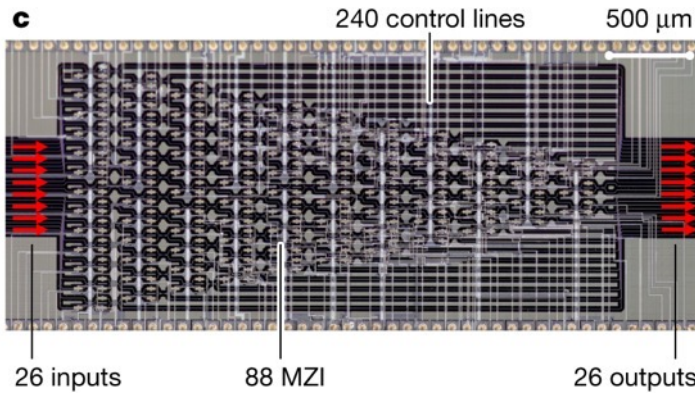


Metasurfaces



Engelberg et al, Nanophotonics (2020)

Photonic Circuits



N. Harris et al, Nature Photonics (2017)

Multi-mode Fibers

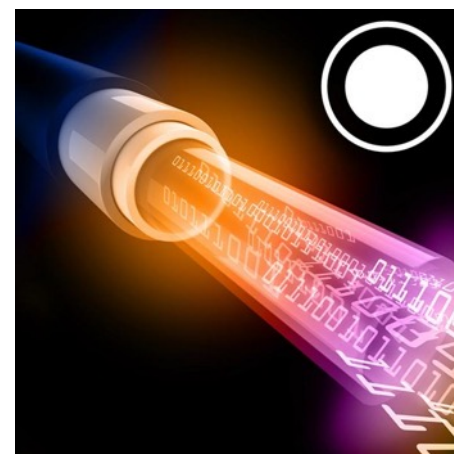
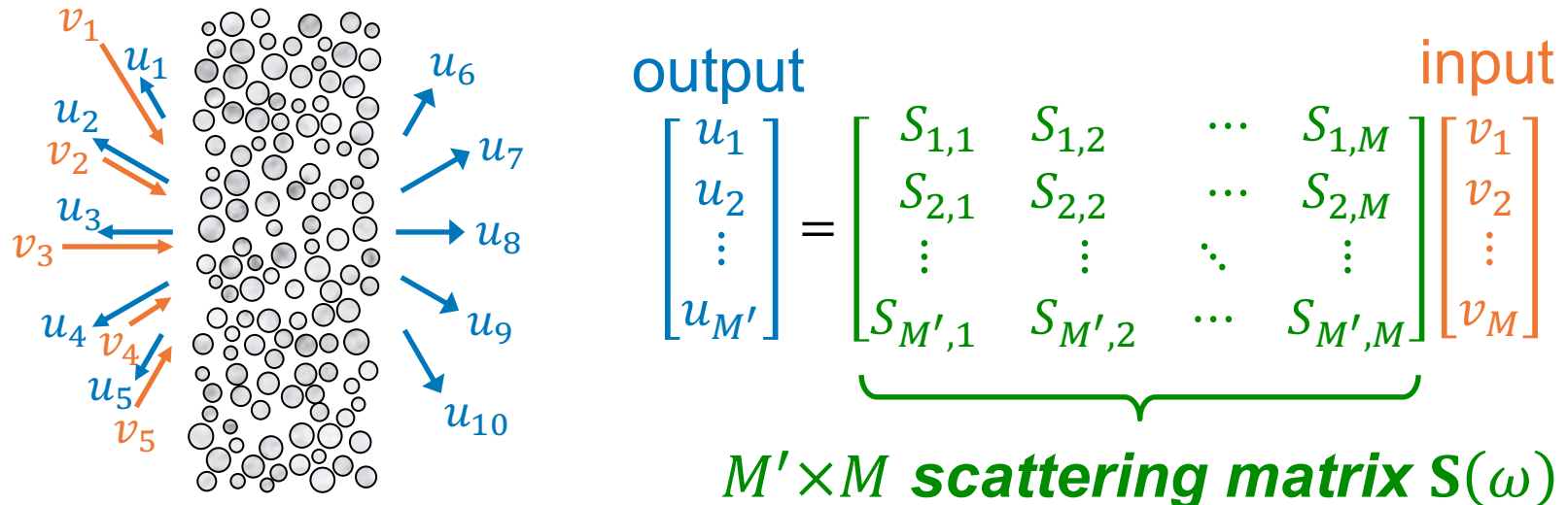


Image from Coherent

The “scattering matrix”



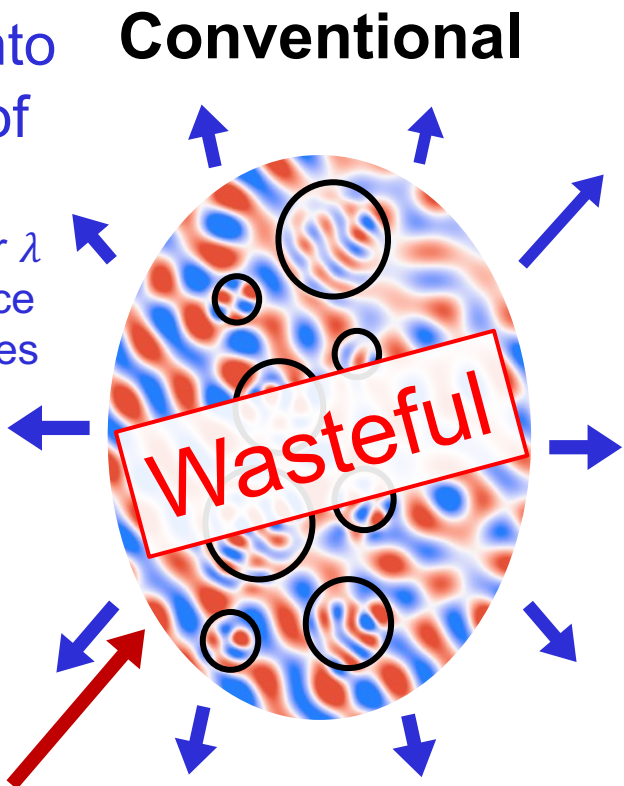
In two-sided systems, $\mathbf{S} = \begin{bmatrix} \mathbf{r} & \mathbf{t}' \\ \mathbf{t} & \mathbf{r}' \end{bmatrix}$, where \mathbf{r} = reflection matrix, \mathbf{t} = transmission matrix.

$\mathbf{S}(\omega)$ fully encapsulates the multi-channel response.

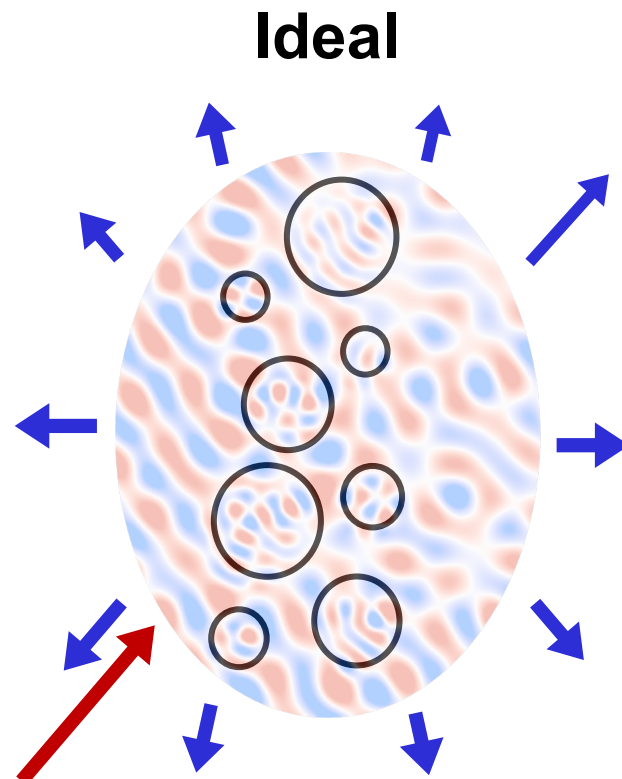
But computing $\mathbf{S}(\omega)$ is a major challenge.

1) Redundancy in field computation

Project onto
outputs of
interest
2 outputs per λ
on the surface
 $\Rightarrow 10$ variables



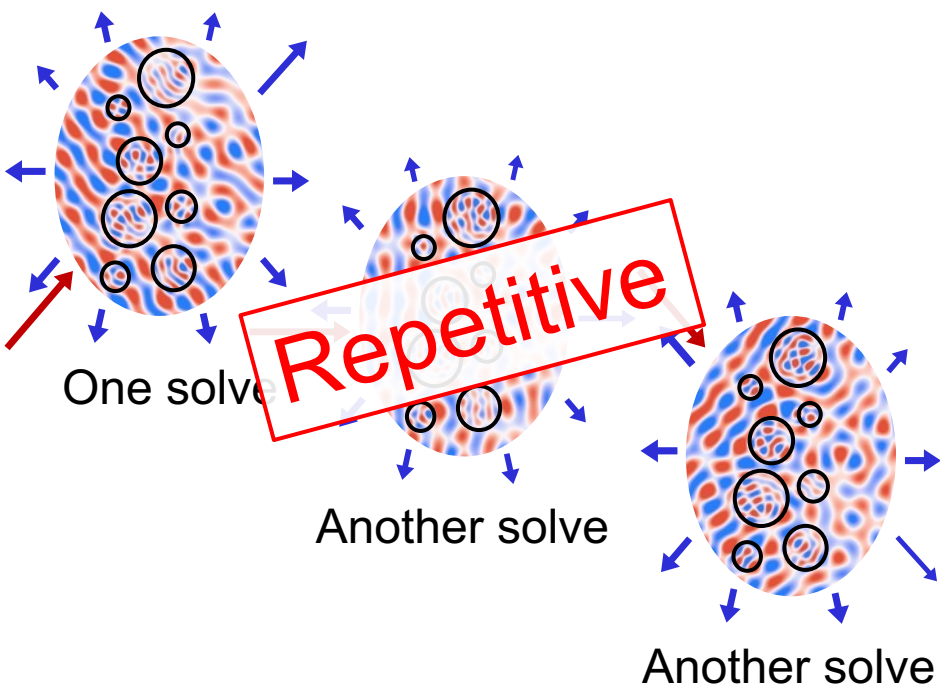
Compute full field profile
20~40 pixels per λ in the volume
 $\Rightarrow 100,000$ variables



Only compute the
outputs of interest

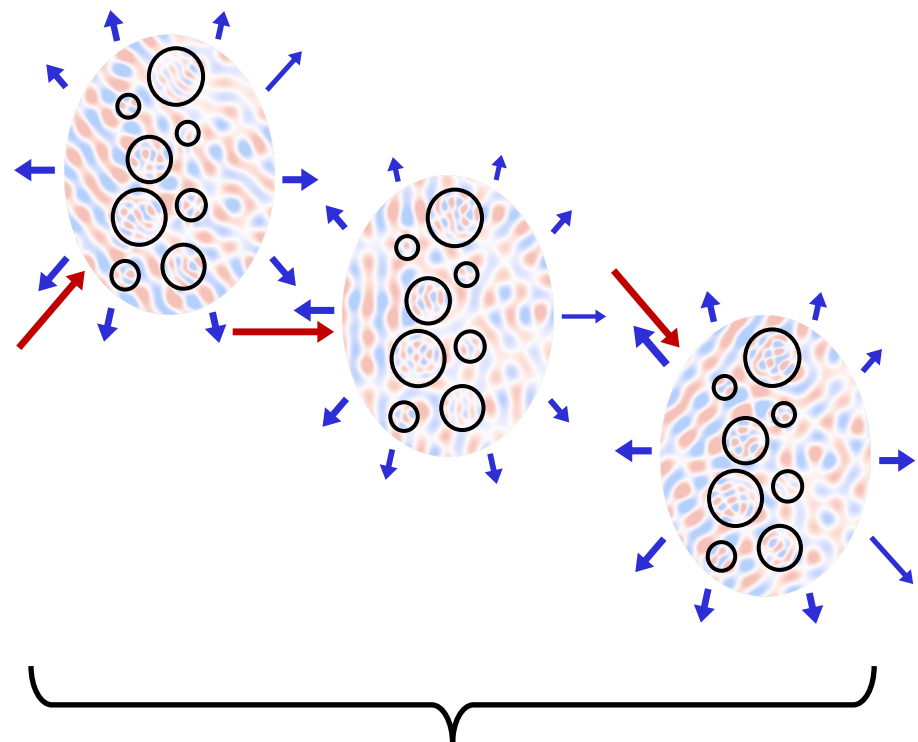
2) Repetitions over inputs

Conventional



Many steps are *repeated*
(when $\text{nrhs} \gg \text{blocking size}$)

Ideal



Outline

1. Augmented partial factorization (APF) method
2. Applications of APF:
 - a) Two-photon coherent backscattering
 - b) Vectorial open channel in 3D
 - c) Noninvasive imaging deep inside scattering media
 - d) Inverse design of metasurfaces

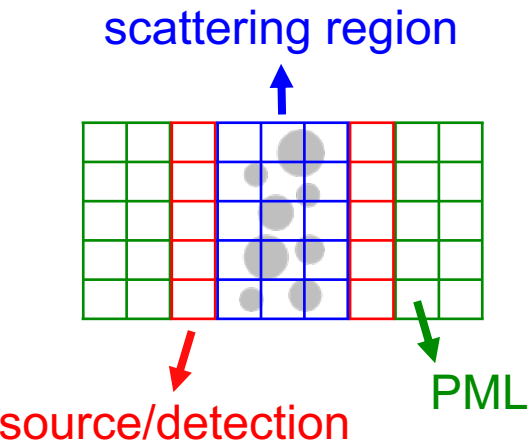
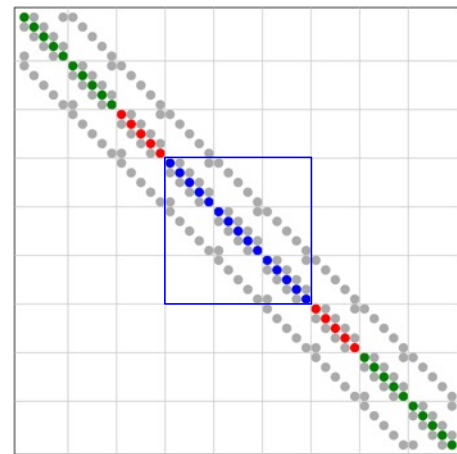
Frequency-domain response problem

Maxwell's equations in frequency domain:

$$\left[-\frac{\omega^2}{c^2} \varepsilon_r(\omega, \mathbf{r}) + \nabla \times \nabla \times \right] \mathbf{E}(\mathbf{r}) = i\omega\mu_0 \mathbf{J}(\mathbf{r})$$

$\underbrace{\phantom{-\frac{\omega^2}{c^2} \varepsilon_r(\omega, \mathbf{r})}}$ $\underbrace{}$ $\underbrace{\phantom{i\omega\mu_0 \mathbf{J}(\mathbf{r})}}$

A
(sparse matrix) **x**
(vector) **b**
(vector)



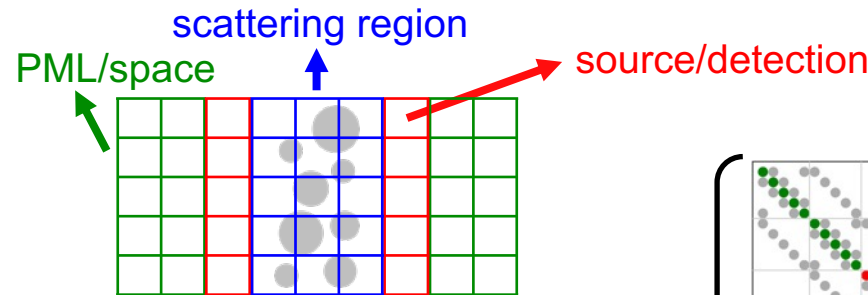
Conventional approach:

1. Factorize $\mathbf{A} = \mathbf{L}\mathbf{U}$
2. Solve for field profile everywhere, $\mathbf{x} = \mathbf{A}^{-1}\mathbf{b}$.
3. Project solution \mathbf{x} onto the outputs of interest.

Sparse system of linear equations: $\mathbf{Ax} = \mathbf{b}$

Repeat for each block of inputs $\{\mathbf{b}\}$

Formulate the generalized scattering matrix



$$\begin{bmatrix} \text{dots} \\ \text{dots} \end{bmatrix} = \begin{bmatrix} \text{dots} \\ \text{dots} \end{bmatrix} \times \begin{bmatrix} \text{dots} \\ \text{dots} \end{bmatrix}$$

Also for thermal emission, LDOS, etc

$$\begin{bmatrix} \text{dots} \\ \text{dots} \end{bmatrix} = \begin{bmatrix} \text{dots} \\ \text{dots} \end{bmatrix} \times \left(\begin{bmatrix} \text{dots} \\ \text{dots} \end{bmatrix}^{-1} \times \begin{bmatrix} \text{dots} \\ \text{dots} \end{bmatrix} - \begin{bmatrix} \text{dots} \\ \text{dots} \end{bmatrix} \right)$$

$A = -\frac{\omega^2}{c^2} \epsilon_r + \nabla \times \nabla \times$

$$S = C \times A^{-1} \times B - D$$

Rows = projection onto the outputs of interest

Columns = different inputs

Columns = full solutions
 $X = A^{-1}B$

Conventional methods

What we want, for any *linear-response problem*

Schur complement

Want an efficient way to evaluate $\mathbf{S} = \mathbf{C} \mathbf{A}^{-1} \mathbf{B} - \mathbf{D}$

projection of \mathbf{A}^{-1} onto \mathbf{C} and \mathbf{B}

Recall a simple problem:

$$ca^{-1}(a x_1 + b x_2 = y_1) \dots \dots \quad (1)$$

$$c x_1 + d x_2 = y_2 \dots \dots \quad (2)$$

Eliminate x_1 . Then solve for x_2

$$\begin{array}{rcl} \cancel{c x_1} + ca^{-1}b x_2 = ca^{-1}y_1 & \dots \dots & ca^{-1}(1) \\ \cancel{c x_1} + d x_2 = y_2 & \dots \dots & (2) \\ \hline (ca^{-1}b - d)x_2 = ca^{-1}y_1 - y_2 & \dots \dots & ca^{-1}(1) - (2) \end{array}$$

Schur complement

Same procedure when we have matrices instead of scalars

Gaussian elimination \Leftrightarrow Eliminate unknowns by projecting them away

Here, want project the \mathbf{A}^{-1} associated with x_1 & y_1 onto x_2 & y_2

\Rightarrow Augment the system, then perform a partial solution

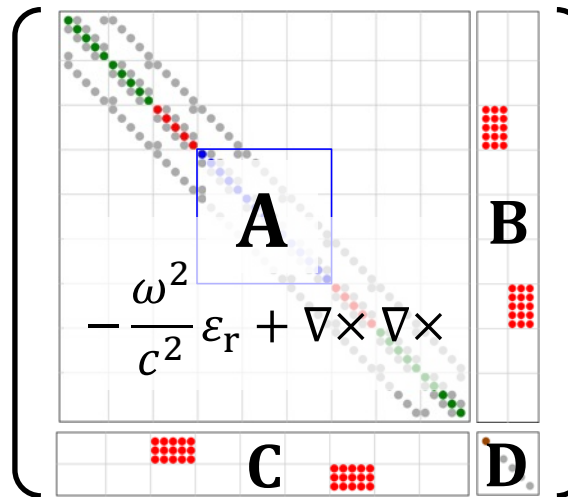
Augmented partial factorization (APF)

Want an efficient way to evaluate $\mathbf{S} = \mathbf{C} \mathbf{A}^{-1} \mathbf{B} - \mathbf{D}$

Step 1:

Build an *augmented matrix*

$$\mathbf{K} = \begin{bmatrix} \mathbf{A} & \mathbf{B} \\ \mathbf{C} & \mathbf{D} \end{bmatrix} =$$



\mathbf{B} = input source profiles

\mathbf{C} = output projection profiles

Step 2: Use MUMPS to compute its Schur complement
(through a partial LU factorization)

$$\mathbf{K} = \begin{bmatrix} \mathbf{A} & \mathbf{B} \\ \mathbf{C} & \mathbf{D} \end{bmatrix} = \begin{bmatrix} \mathbf{L} & \mathbf{0} \\ \mathbf{E} & \mathbf{I} \end{bmatrix} \begin{bmatrix} \mathbf{U} & \mathbf{F} \\ \mathbf{0} & \mathbf{H} \end{bmatrix}$$

Schur complement

Step 3: Return $-\mathbf{H} = \mathbf{C} \mathbf{A}^{-1} \mathbf{B} - \mathbf{D} = \mathbf{S}$

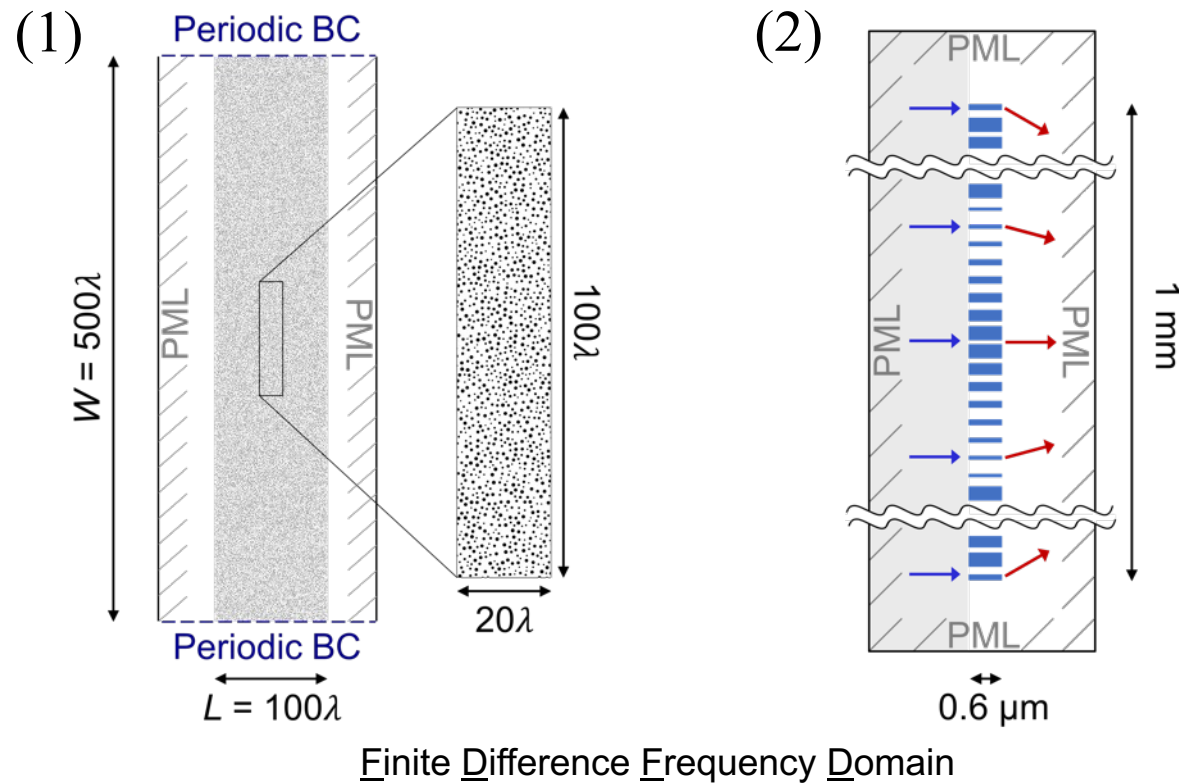
Solves for all inputs using a single factorization!

Augmented partial factorization (APF) advantages

- ✓ Full-wave solution; no approximation beyond discretization
- ✓ **Does not compute unnecessary solution, i.e. $\mathbf{X} = \mathbf{A}^{-1}\mathbf{B}$**
- ✓ **A single partial factorization solves M scattering problems with different inputs**
- ✓ Can use MUMPS \Rightarrow Optimized & scalable for parallel computing
- ✓ Does not need **L** and **U** factors [ICNTL(31)=1] \Rightarrow saves memory
- ✓ Uses all sparsity properties of **A**, **B**, **C** (up to a factor of 4)
- ✓ Applicable to **any linear system**:
 - ✓ Any structure $\varepsilon_r(\omega, \mathbf{r})$ including substrate etc; any dispersion
 - ✓ Any input sources & any output projections
 - ✓ Any linear PDE & any discretization scheme
(finite difference, finite element, boundary element, ...)
 - ✓ Any linear problem of the form **C A⁻¹ B**

Benchmarks on large-scale multi-channel systems

Implemented APF with finite difference on Yee grid



Compare: APF, Direct^[1] & iterative^[2] FDFD, RCWA^[3], RGF^[4]:

[1] MaxwellFDFD: <https://github.com/wsshin/maxwellfdfd>

[2] FD3D: <https://github.com/wsshin/fd3d>

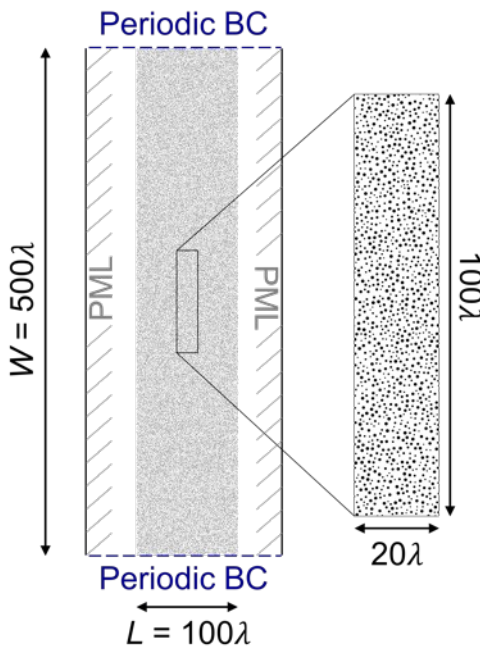
[3] S4: <https://github.com/victorliu/S4>

[4] RGF: <https://github.com/chiaweihsu/RGF>

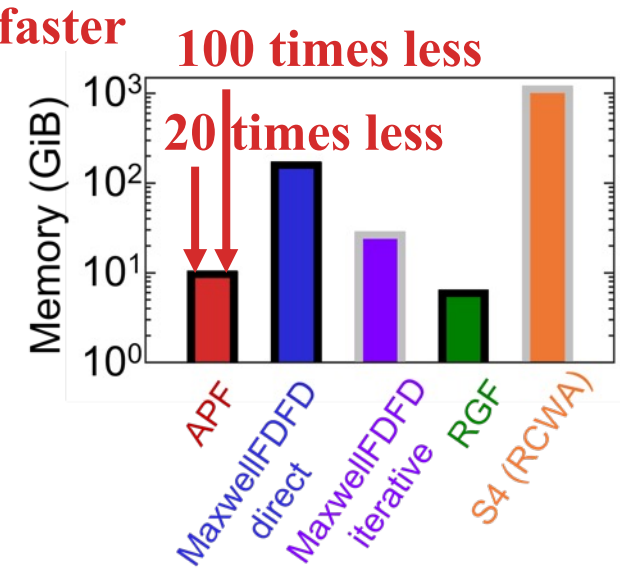
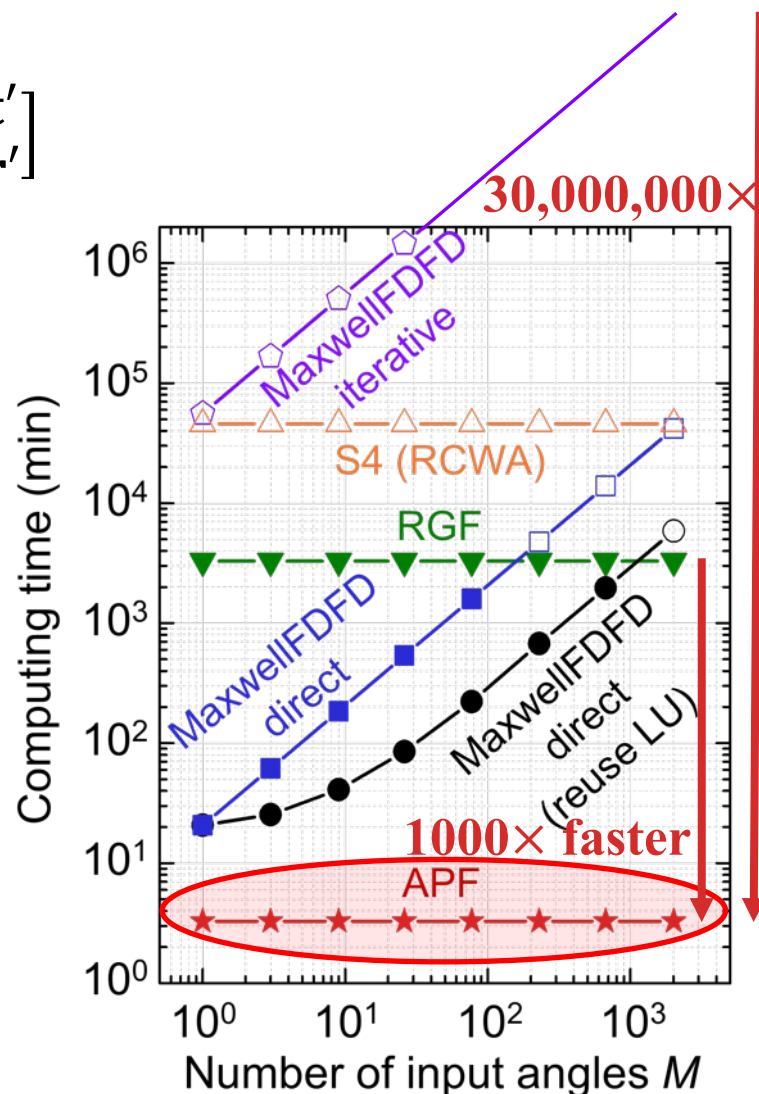
2D TM waves
Uses **MUMPS** for partial factorization
On Intel Xeon Gold 6130 (using 1 core)

Benchmark 1: disordered media

$$\text{Compute } S = \begin{bmatrix} \mathbf{r} & \mathbf{t}' \\ \mathbf{t} & \mathbf{r}' \end{bmatrix}$$



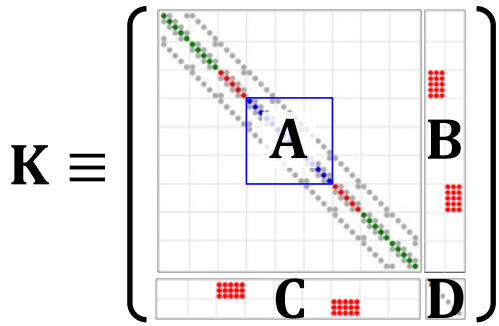
30,000 scatterers
12 million pixels
(resolution: $\Delta x = \lambda/15$)



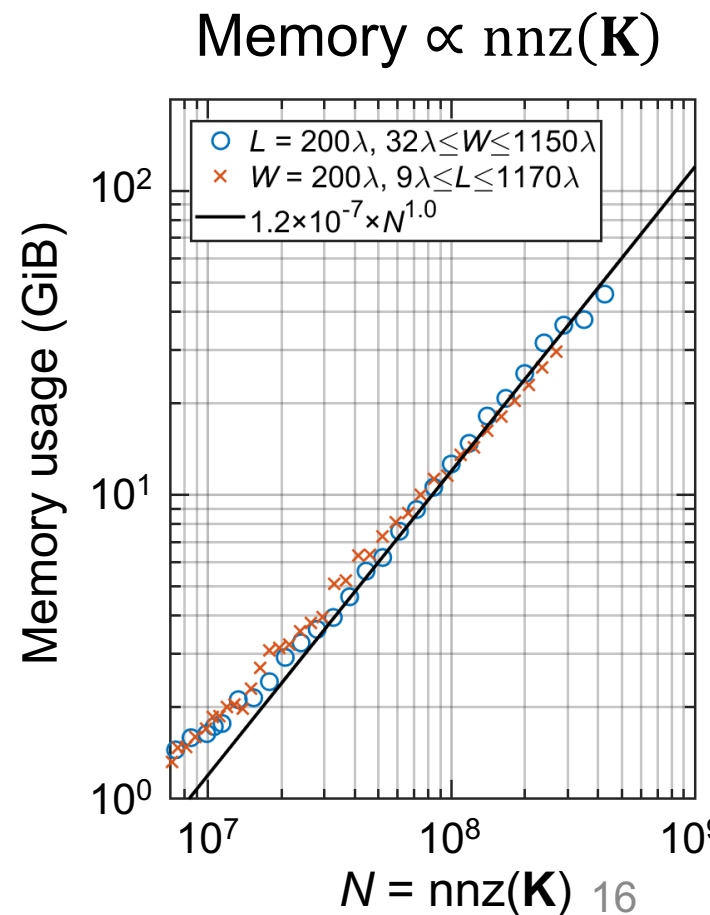
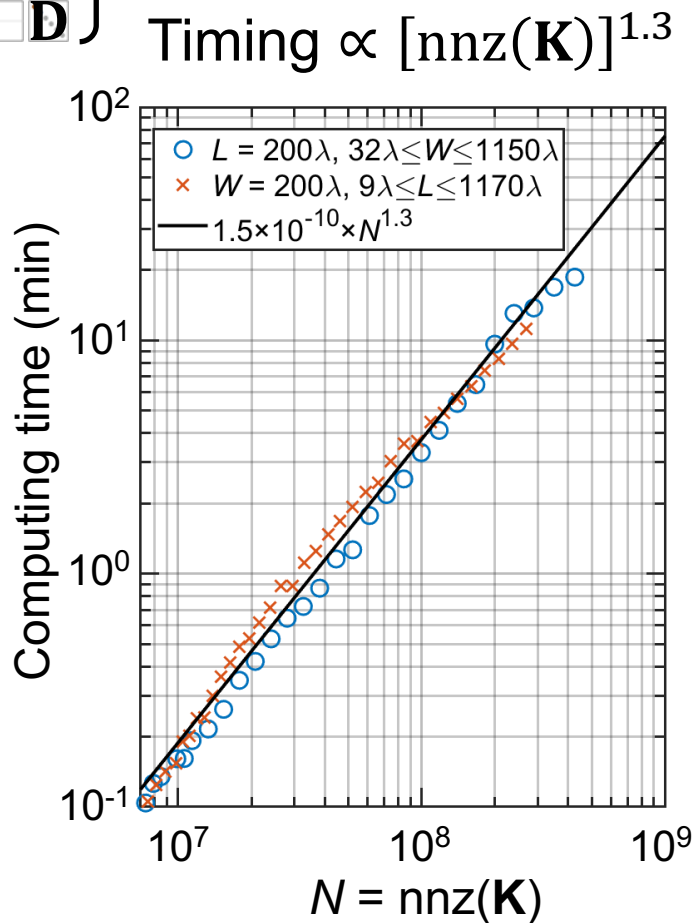
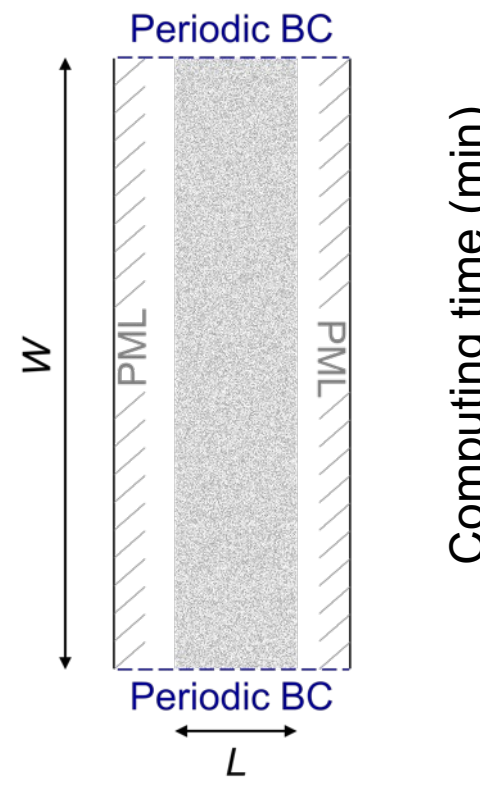
Time breakdown of APF



Computing time & memory usage scaling in 2D

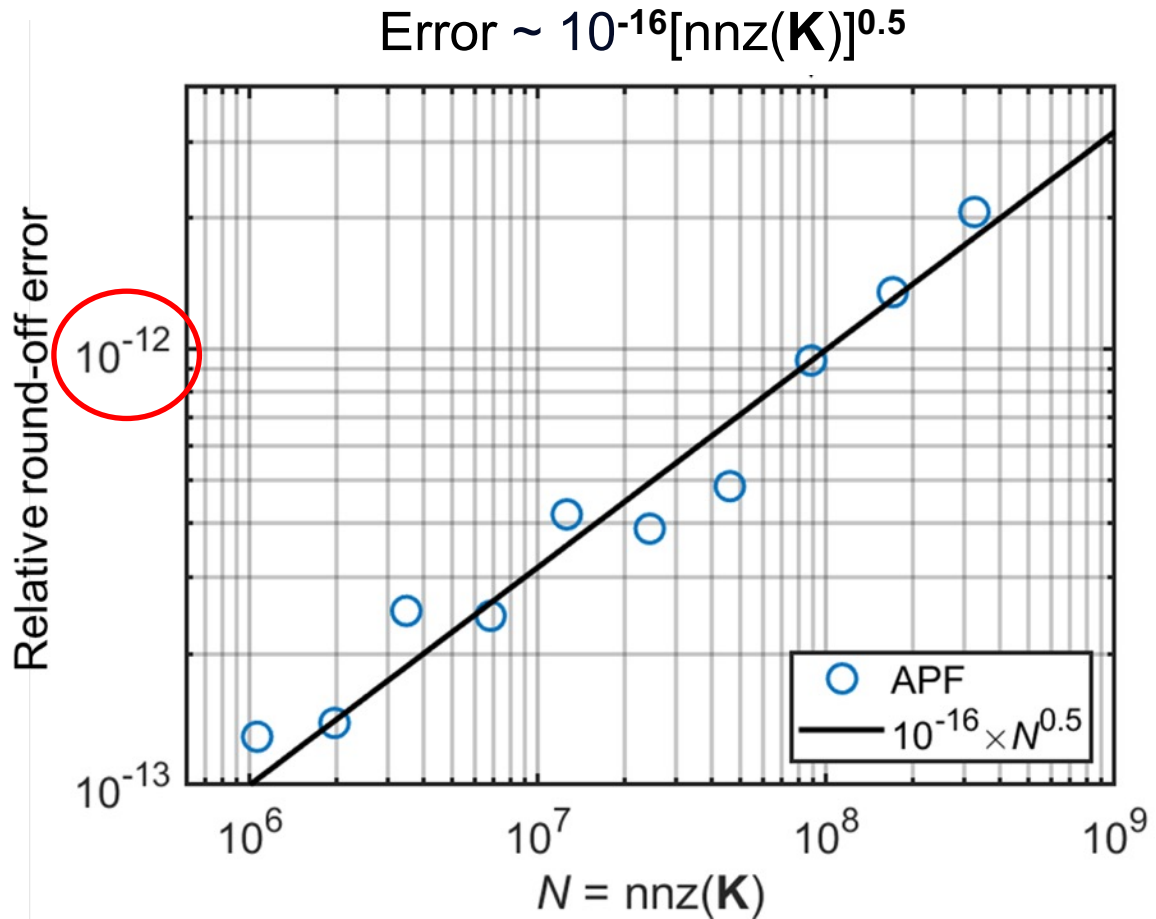
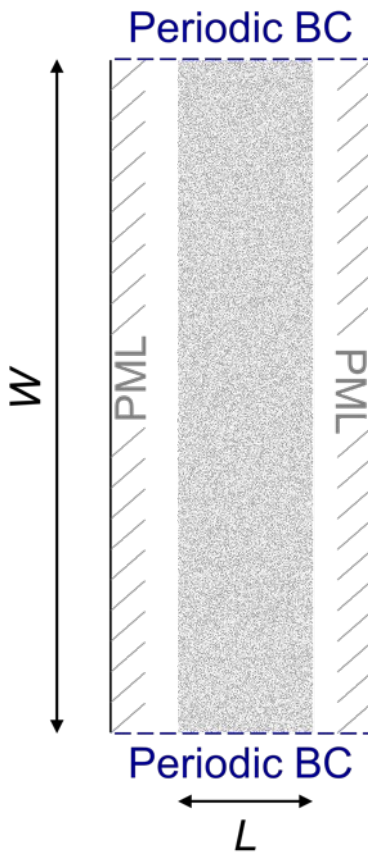


Timing & memory are governed primarily by the number of non-zero elements, $\text{nnz}(\mathbf{K})$.
 $\text{nnz}(\mathbf{K}) \propto$ system size



Numerical round-off error

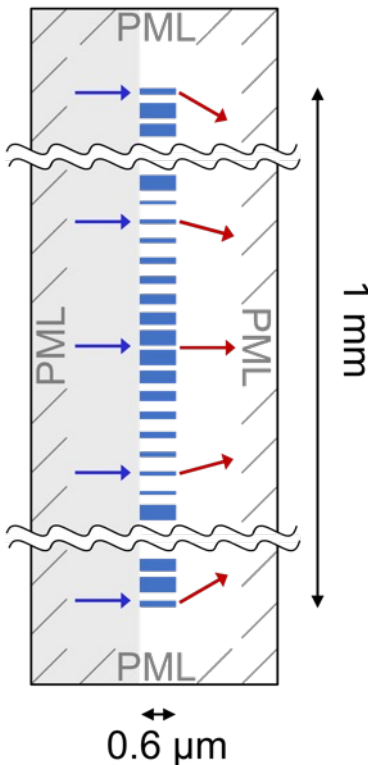
(double-precision arithmetic)
(no iterative refinement)



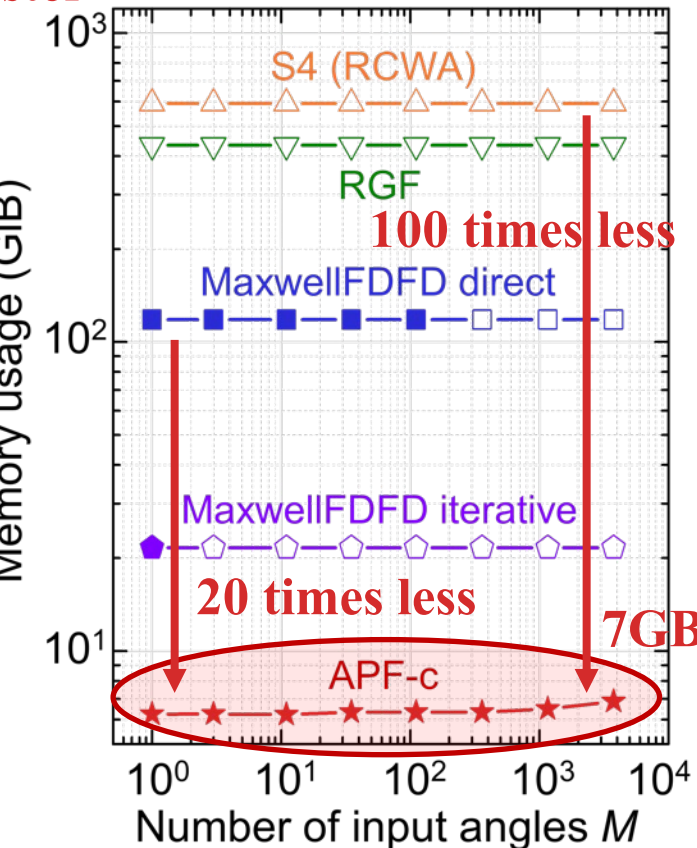
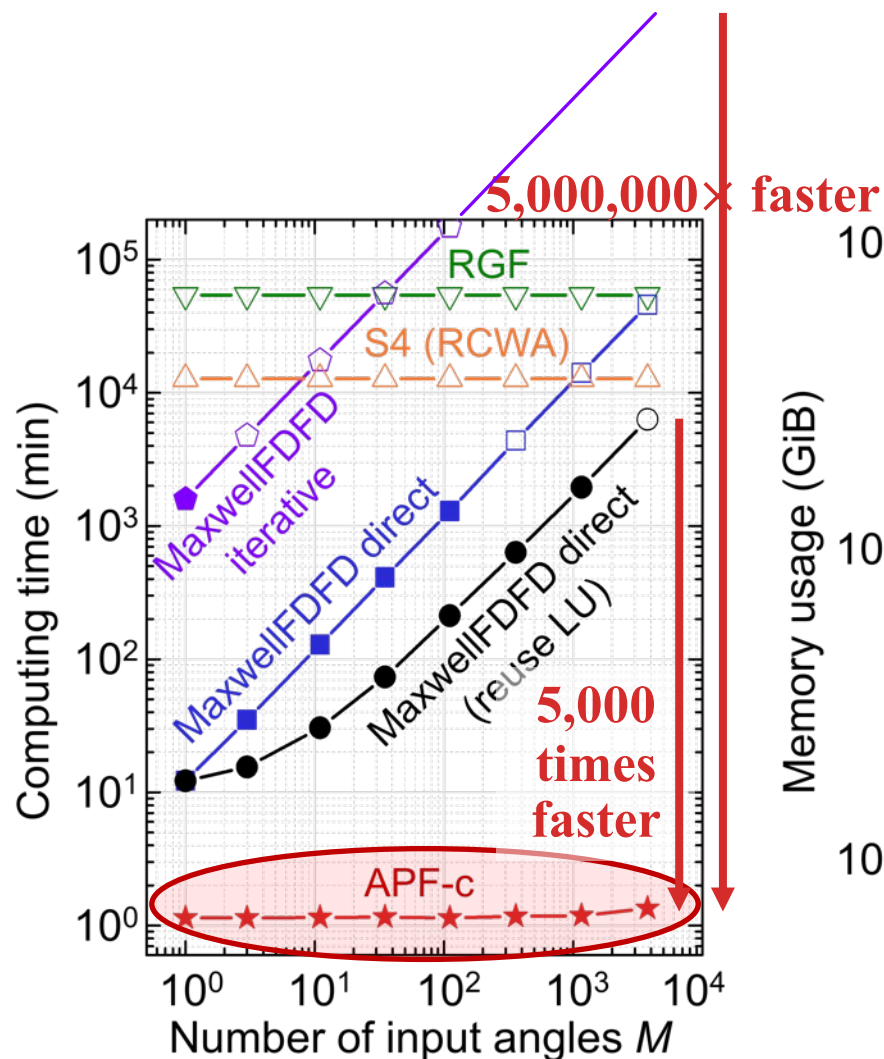
Only relevant error is from discretization

Benchmark 2: mm-scale TiO_2 metlens

Compute t

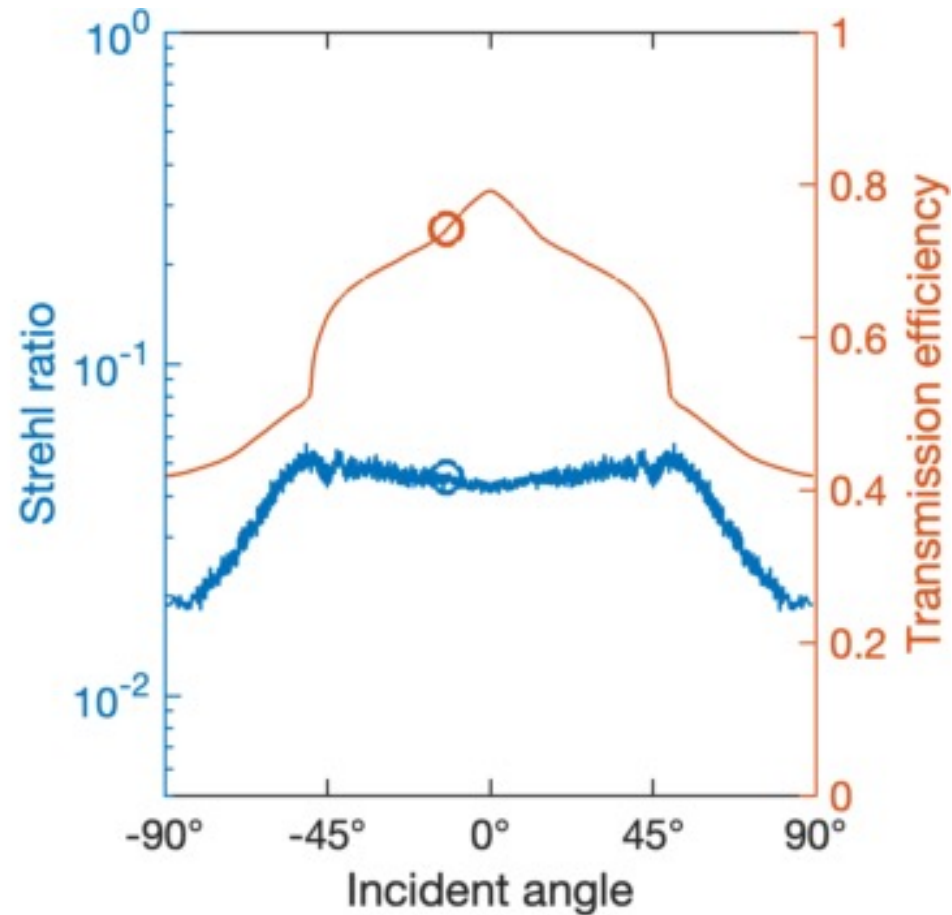
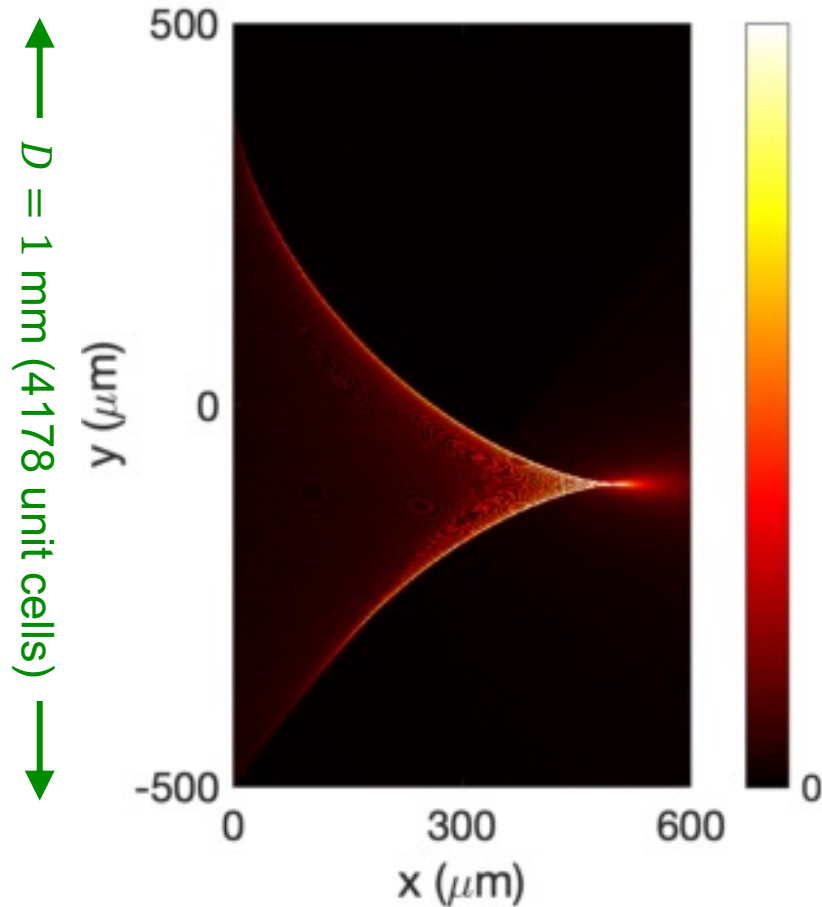


4,178 unit cells
11 million pixels
(resolution: $\Delta x = \lambda/40$; $\lambda = 532 \text{ nm}$)



Example: High-NA quadratic metalens

$$\phi(\rho) = -\frac{2\pi}{\lambda} \frac{\rho^2}{2f} \quad (D = 1000 \text{ } \mu\text{m}, f = 500 \text{ } \mu\text{m, NA} = 0.71)$$



Full-wave simulation @ 3,761 incident angles

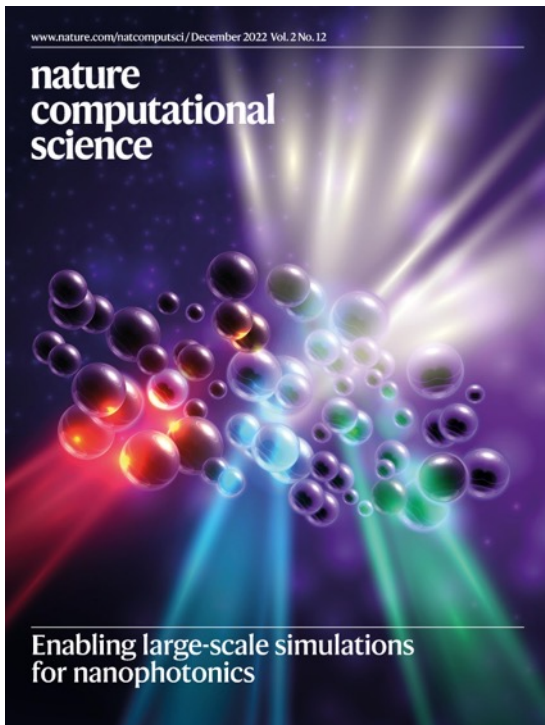
Total computing time ~ 1 minute using one core on a laptop

MESTI software

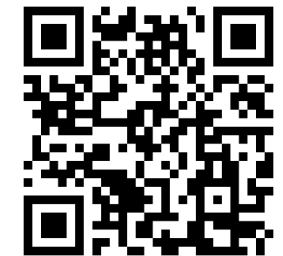
Maxwell's Equations Solver with Thousands of Inputs

<https://github.com/complexphoton/MESTI.m>

Uses sequential MUMPS (yes multithreading, no MPI)



- Open-source
- TE & TM polarizations in 2D
- Any $\epsilon(x, y)$ including substrates etc
- Any dispersion
- Any list of input source profiles
- Any list of output projection profiles (or full solution)
- All common boundary conditions
- PML with real & imaginary coordinate stretching
- Utility functions for building inputs/outputs
- Documentation
- Examples



3D vectorial version in Julia using parallel MUMPS: coming soon!

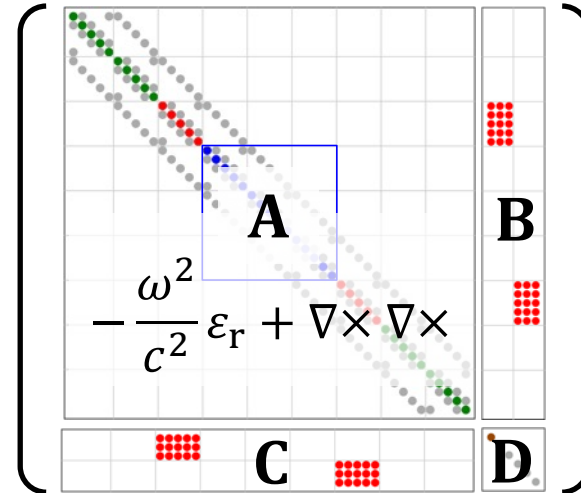
One caveat

Want to evaluate $\mathbf{S} = \mathbf{C} \mathbf{A}^{-1} \mathbf{B} - \mathbf{D}$

Step 1:

Build an *augmented matrix*

$$\mathbf{K} \equiv \begin{bmatrix} \mathbf{A} & \mathbf{B} \\ \mathbf{C} & \mathbf{D} \end{bmatrix} =$$



\mathbf{B} = input source profiles

\mathbf{C} = output projection profiles

Step 2: Compute its Schur complement

$$\mathbf{K} \equiv \begin{bmatrix} \mathbf{A} & \mathbf{B} \\ \mathbf{C} & \mathbf{D} \end{bmatrix} = \begin{bmatrix} \mathbf{L} & \mathbf{0} \\ \mathbf{E} & \mathbf{I} \end{bmatrix} \begin{bmatrix} \mathbf{U} & \mathbf{F} \\ \mathbf{0} & \mathbf{H} \end{bmatrix}$$

Schur complement

Step 3: Return $-\mathbf{H} = \mathbf{C} \mathbf{A}^{-1} \mathbf{B} - \mathbf{D} = \mathbf{S}$

What if number of columns in $\mathbf{B} \neq$ number of rows in \mathbf{C} ?

⇒ Pad zero-columns to \mathbf{B} or zero-rows to \mathbf{C}

Very inefficient when the two numbers are very different (eg: gradient)

Wish list for MUMPS: skip Schur complement evaluation associated with zero rows/columns

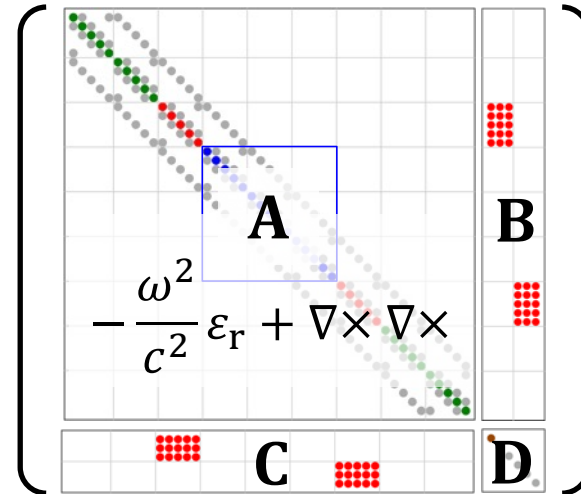
Schur complement without LU?

Want to evaluate $\mathbf{S} = \mathbf{C} \mathbf{A}^{-1} \mathbf{B} - \mathbf{D}$

Step 1:

Build an *augmented matrix*

$$\mathbf{K} \equiv \begin{bmatrix} \mathbf{A} & \mathbf{B} \\ \mathbf{C} & \mathbf{D} \end{bmatrix} =$$



\mathbf{B} = input source profiles

\mathbf{C} = output projection profiles

Step 2: Compute its Schur complement

$$\mathbf{K} \equiv \begin{bmatrix} \mathbf{A} & \mathbf{B} \\ \mathbf{C} & \mathbf{D} \end{bmatrix} = \begin{bmatrix} \mathbf{L} & \mathbf{0} \\ \mathbf{E} & \mathbf{I} \end{bmatrix} \begin{bmatrix} \mathbf{U} & \mathbf{F} \\ \mathbf{0} & \mathbf{H} \end{bmatrix}$$

Schur complement

Step 3: Return $-\mathbf{H} = \mathbf{C} \mathbf{A}^{-1} \mathbf{B} - \mathbf{D} = \mathbf{S}$

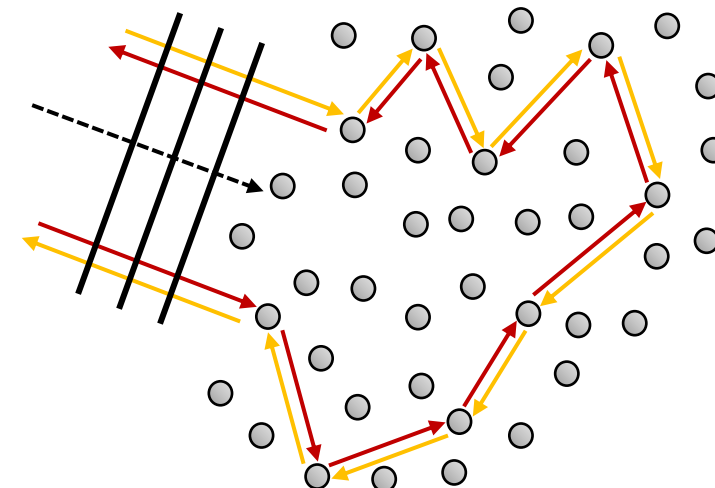
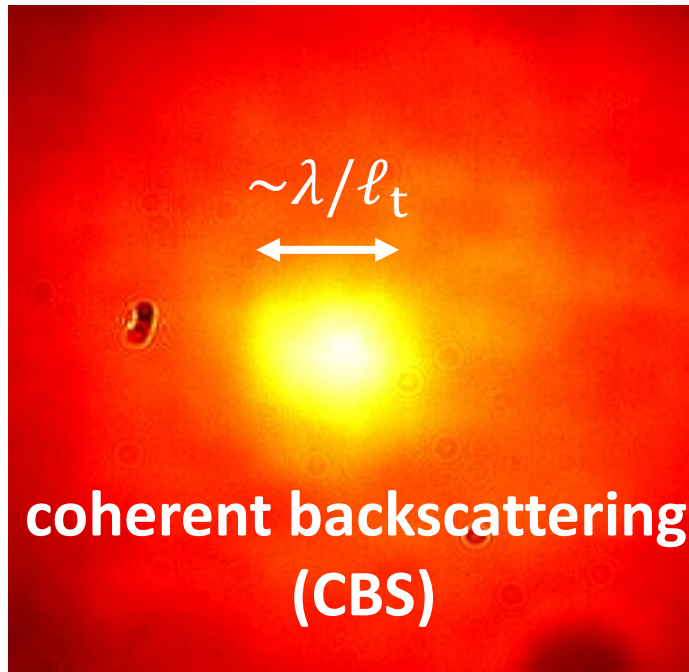
We only need the Schur complement; not the LU factors
⇒ Potential room for further acceleration?

Outline

1. Augmented partial factorization (APF) method
2. Applications of APF (all done with MESTI):
 - a) Two-photon coherent backscattering
with Yaron Bromberg @ Hebrew University
& Arthur Goetschy @ Institut Langevin
 - b) Vectorial open channel in 3D
 - c) Noninvasive imaging deep inside scattering media
 - d) Inverse design of metasurfaces

Coherent backscattering (CBS) of classical light

Disorder averaged backscattered intensity



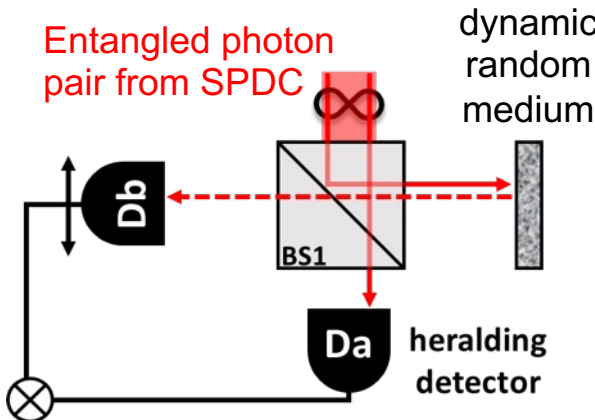
ℓ_t : transport mean free path

Akkermans, Wolf, Maynard, PRL (1986)

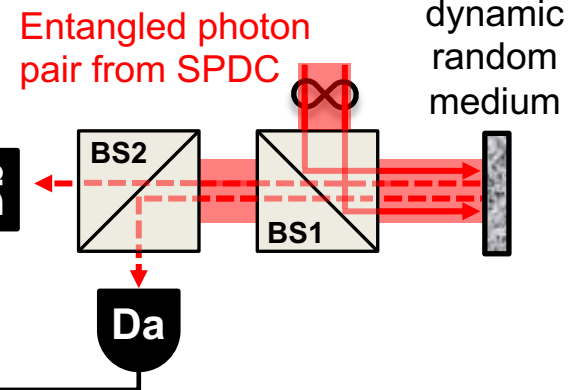
**Does non-classical light exhibit CBS?
How does that differ from classical CBS?**

Coherent backscattering of non-classical light

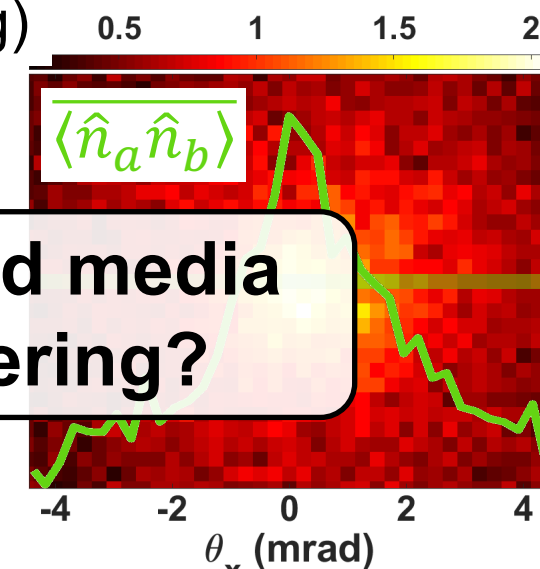
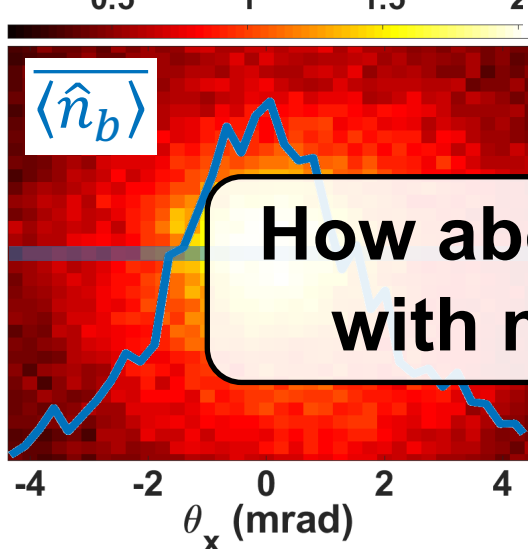
One-photon CBS



Two-photon CBS



(double scattering)



How about disordered media
with multiple scattering?

Theory of two-photon CBS

Entangled photon-pair input: $|\psi\rangle \propto \sum_{q'} \hat{c}_{q'}^\dagger \hat{c}_{-q'}^\dagger |0\rangle$

\hat{c}_q^\dagger : creation operator
for input mode

Reflected output: $\hat{d}_q = \sum_{q'} r_{qq'} \hat{c}_{q'}$ $r_{qq'}$: reflection matrix

Coincidence rate $\propto \frac{\langle \psi | : \hat{n}_a \hat{n}_b : | \psi \rangle}{\langle (\hat{r}^2)_{q_b, -q_a} \rangle^2}$ $\hat{n}_q = \hat{d}_q^\dagger \hat{d}_q$ — disorder average
matrix square (use reciprocity)

Need:

- Full reflection matrix r for all of the many input/output angles.
- Average over thousands of disorder realizations.
- System width $W \gtrsim 60\ell_t$ to resolve the two-photon CBS cone.
- System thickness $L \gg \ell_t$ to be in diffusive regime of transport.
- Need to suppress single scattering in reflection \Rightarrow ~~point scatterers~~
- Full-wave solution.

Very challenging for existing numerical methods...

But not with APF.

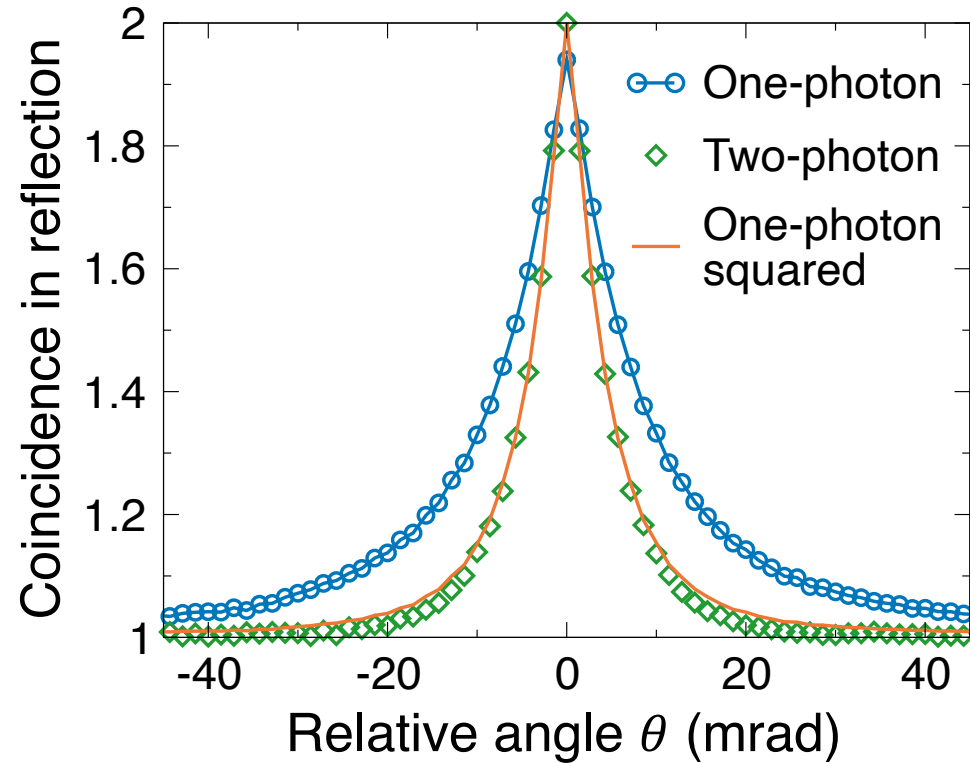
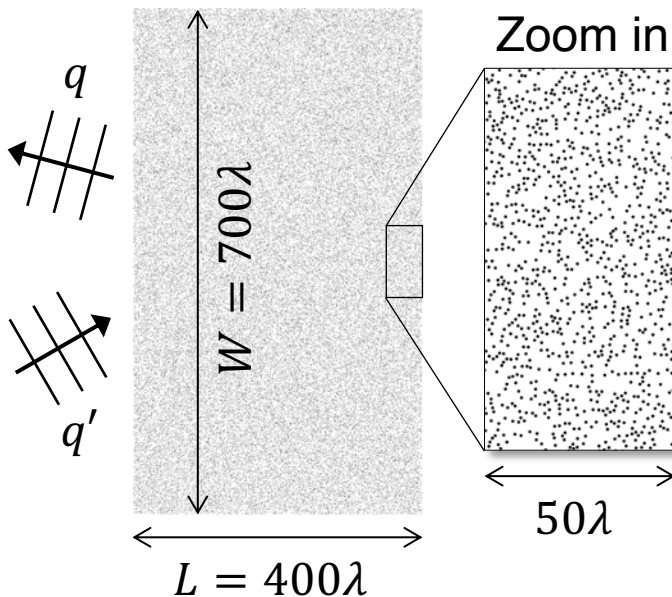
Two-photon CBS in disordered media

56,000 scatterers

28 million pixels

(resolution: $\Delta x = \lambda/10$)

1,400 angles per side



Compute 4,000 reflection matrices from 2,000 realizations

One realization takes 11 minutes using one core, using APF

Outline

1. Augmented partial factorization (APF) method
2. Applications of APF:
 - a) Two-photon coherent backscattering
 - b) **Vectorial open channel in 3D**
 - c) Noninvasive imaging deep inside scattering media
 - d) Inverse design of metasurfaces

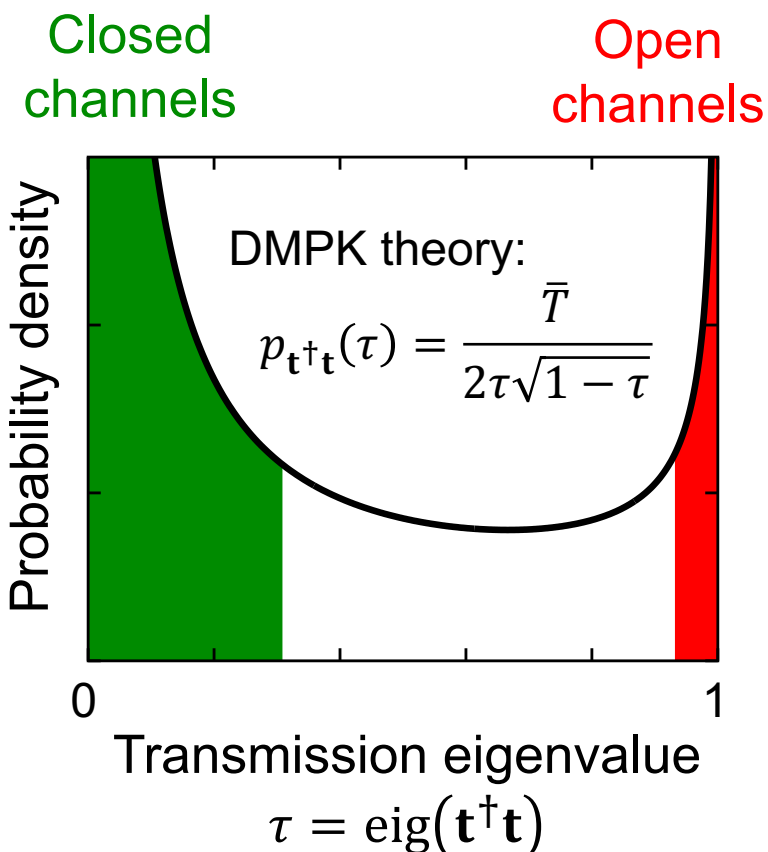
Open channels through disorder

First predicted for scalar electron waves:

Dorokhov, *Solid State Commun* (1984)

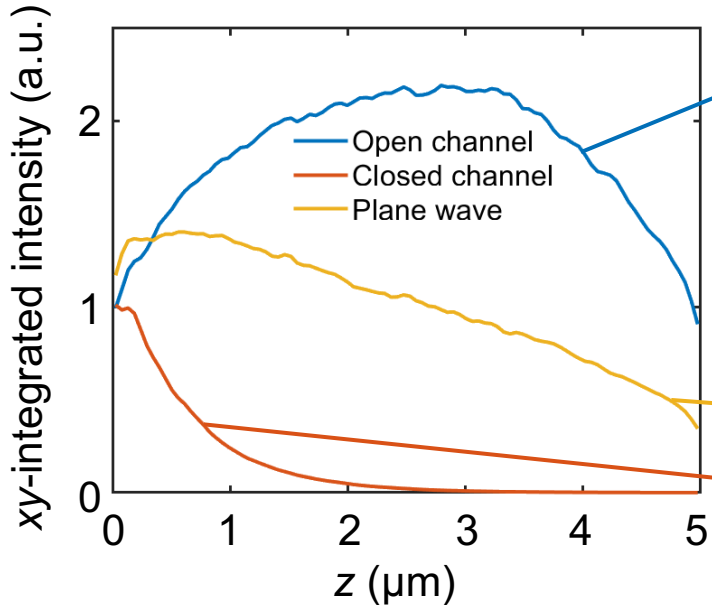
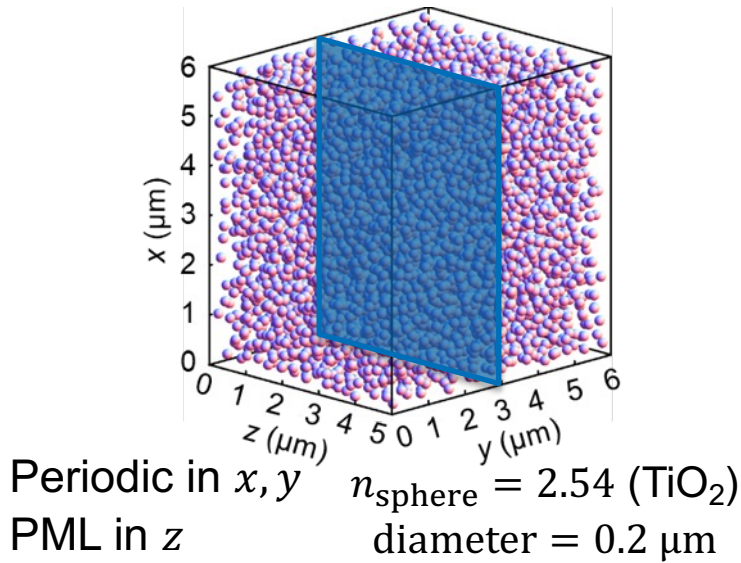
Mello, Pereyra, Kumar, *Ann Phys* (1988)

$$S = \begin{bmatrix} \mathbf{r} & \mathbf{t}' \\ \mathbf{t} & \mathbf{r}' \end{bmatrix} \text{ for two-sided systems}$$

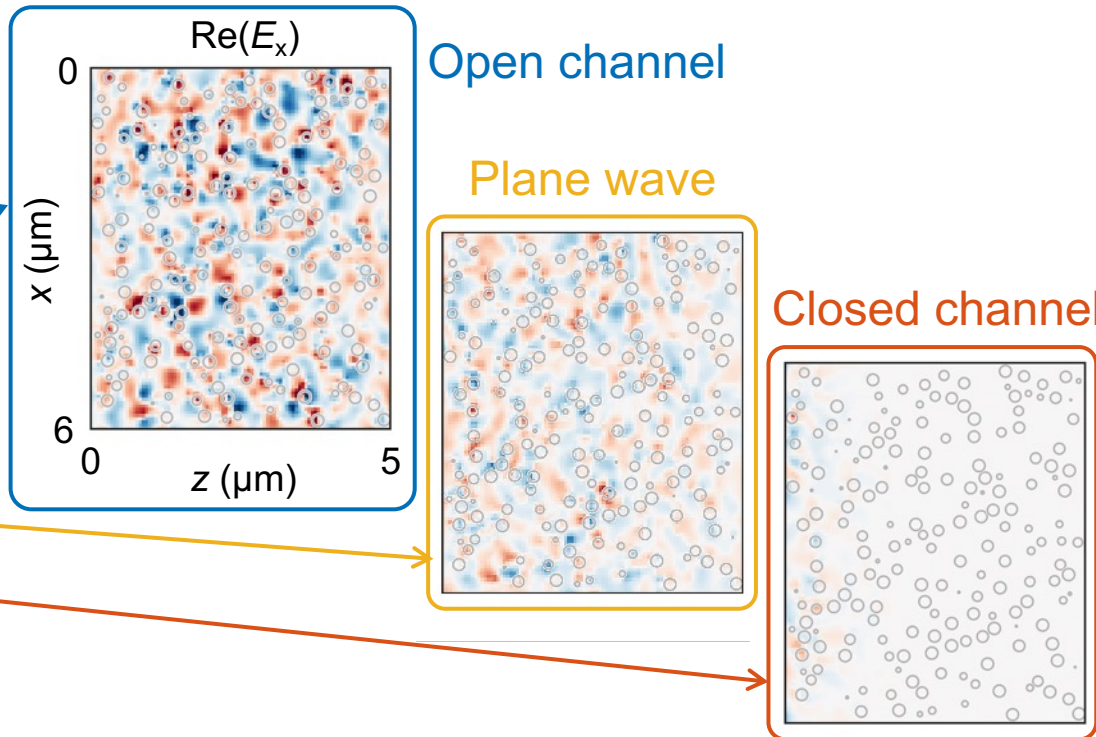


- Shaping the wavefront of electrons is hard.
- Realized for scalar waves in 2D waveguides:
 - FDTD simulation: Choi et al, *PRB* (2011)
 - Acoustic exp: Gérardin et al, *PRL* (2014)
 - Optical exp: Sarma et al, *PRL* (2016)
 - Microwave exp: Horodynski et al, *Nature* (2022)
- Realization in 3D remains challenging:
 - Experiments face incomplete channel control
 - Yu et al, *PRL* (2013): 7% \Rightarrow 65%
 - Popoff et al, *PRL* (2014): 5% \Rightarrow 18%
 - Bosch, PhD thesis (2020): 26% \Rightarrow 49%
 - Simulations take unrealistic resources (but not with APF!)

Open channel for 3D vectorial EM waves



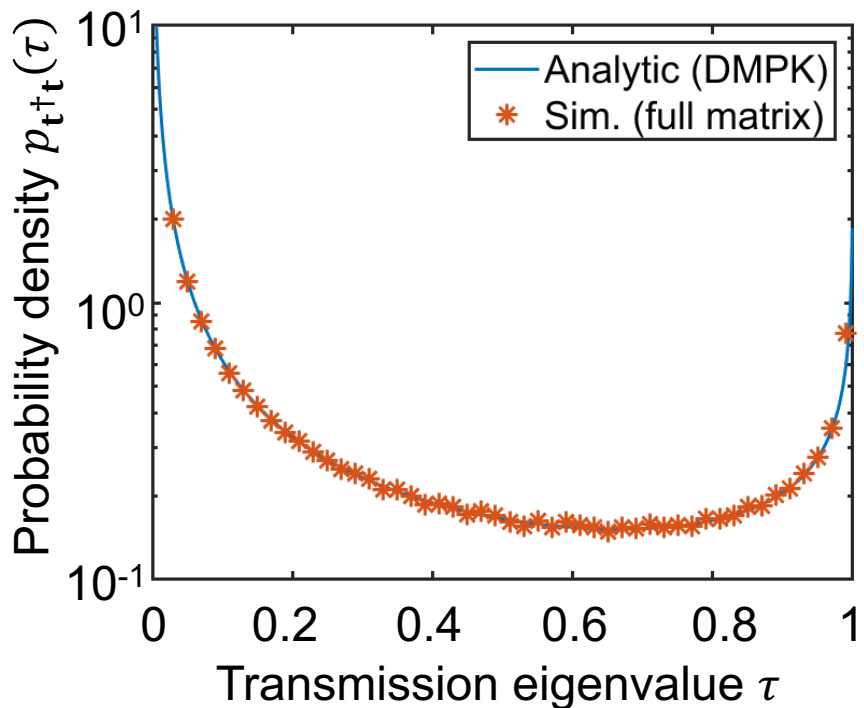
6,000 scatterers; 2 million voxels
 $\lambda = 532 \text{ nm}; \Delta x = \lambda/10$
 $\bar{T} = 0.12; g \approx 100$
826 angles per side (both polarizations)
APF computation takes 25 minutes (using one 16-core Intel Xeon Gold 6130)
Memory: 87 GB (would be 300 GB if LU is stored)



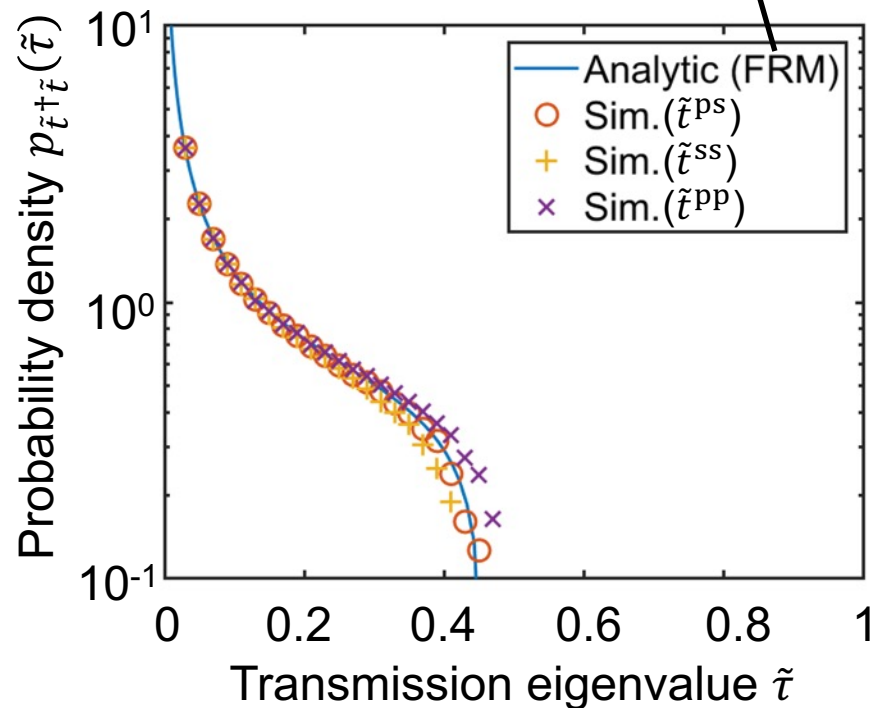
Eigenvalue distribution for 3D vectorial EM waves

Filtered random matrix (FRM) theory
A. Goetschy & A. D. Stone, PRL (2013)

Full transmission matrix



One-quarter of t

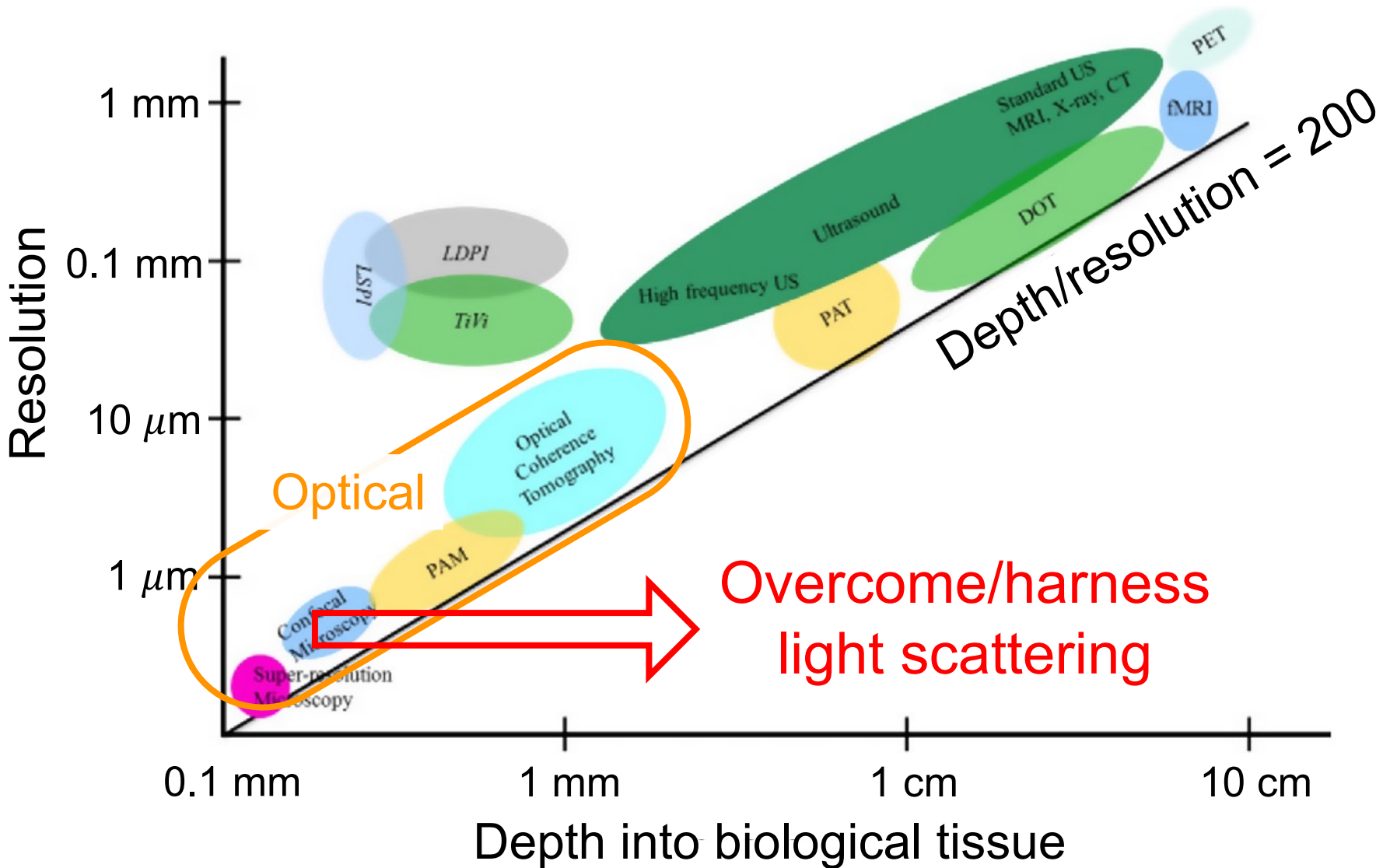


Ensemble average over 500 realizations

Outline

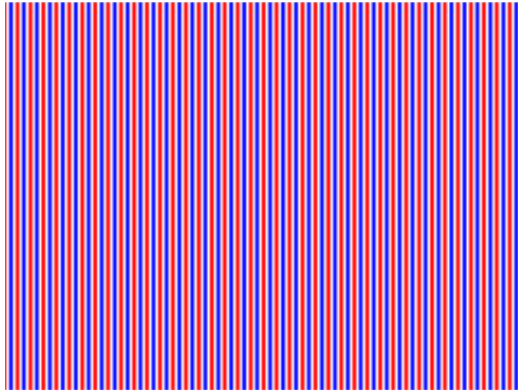
1. Augmented partial factorization (APF) method
2. Applications of APF:
 - a) Two-photon coherent backscattering
 - b) Vectorial open channel in 3D
 - c) Noninvasive imaging deep inside scattering media
 - d) Inverse design of metasurfaces

Depth-vs-resolution trade-off for deep imaging

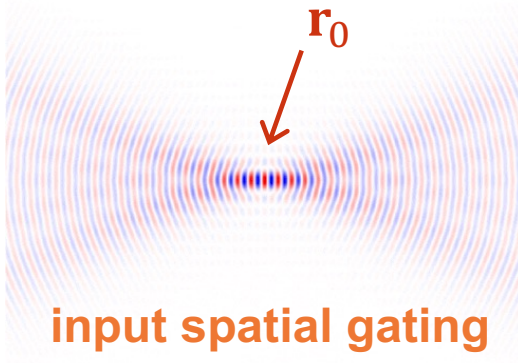


Spatiotemporal gating \Leftrightarrow summing plane waves

$$e^{i\mathbf{k}_{in} \cdot (\mathbf{r} - \mathbf{r}_0) - i\omega t}$$



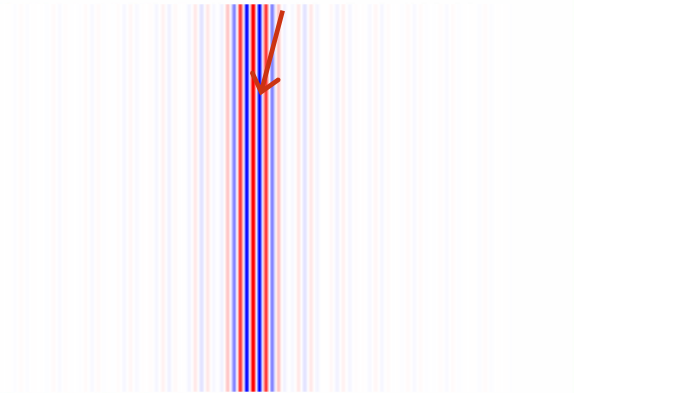
$$\sum_{\mathbf{k}_{in}} e^{i\mathbf{k}_{in} \cdot (\mathbf{r} - \mathbf{r}_0) - i\omega t}$$



input spatial gating

$$\sum_{\omega} e^{i\mathbf{k}_{in} \cdot (\mathbf{r} - \mathbf{r}_0) - i\omega t}$$

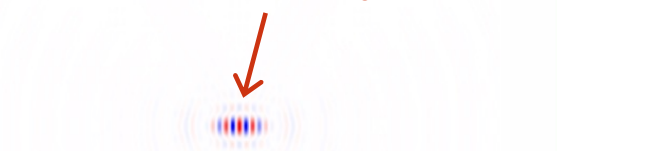
arrive at \mathbf{r}_0 at time $t = 0$



time gating

$$\sum_{\omega} \sum_{\mathbf{k}_{in}} e^{i\mathbf{k}_{in} \cdot (\mathbf{r} - \mathbf{r}_0) - i\omega t}$$

arrive at \mathbf{r}_0 at time $t = 0$

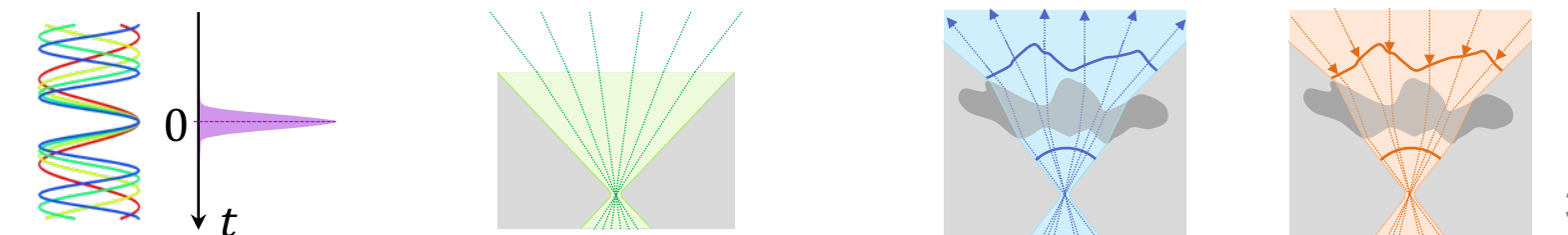
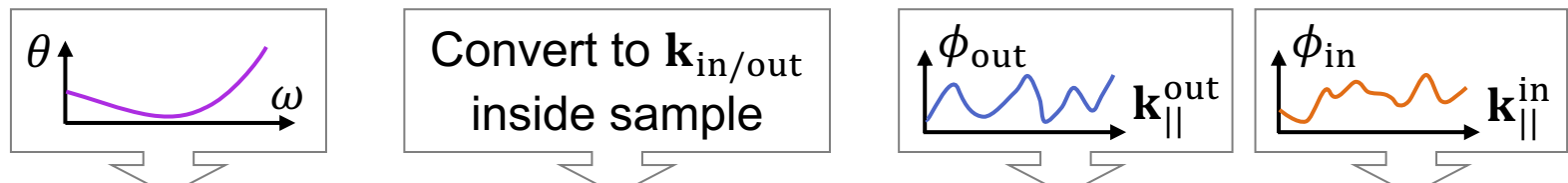
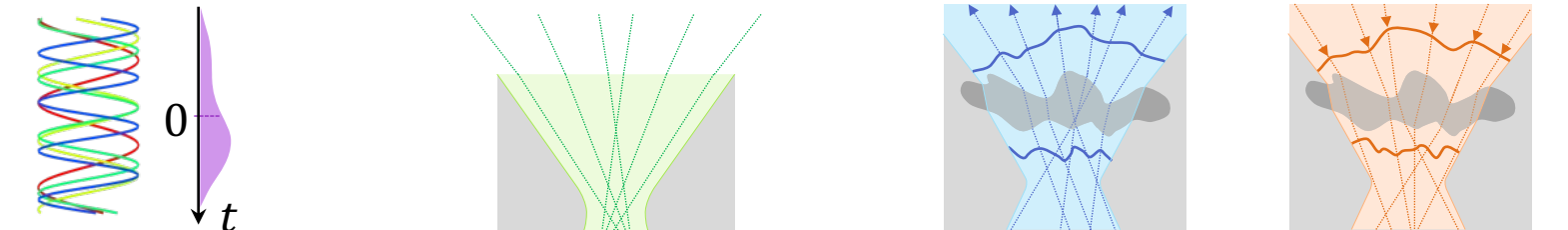
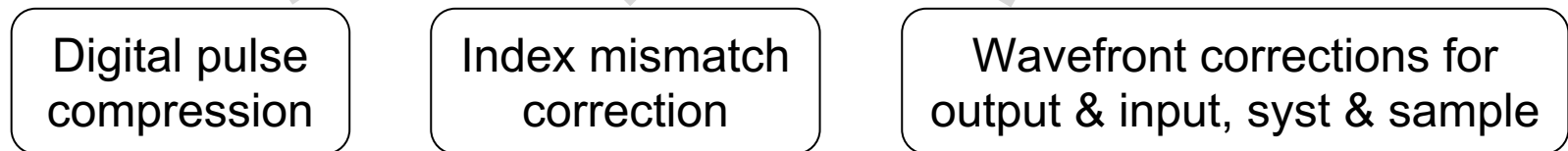


spatio-temporal gating

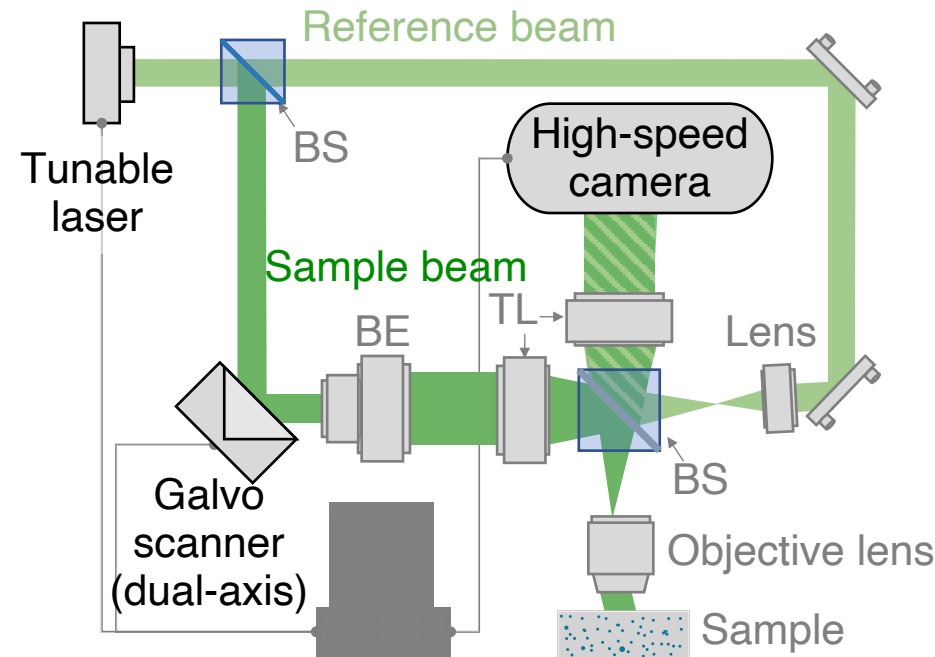
Scattering matrix tomography (SMT)

$$I_{\text{SMT}}(\mathbf{r}) = \left| \sum_{\omega} e^{i \theta(\omega)} \sum_{\mathbf{k}_{\text{out}}} e^{i \mathbf{k}_{\text{out}} \cdot \mathbf{r} + i \phi_{\text{out}}(\mathbf{k}_{\text{out}})} \sum_{\mathbf{k}_{\text{in}}} e^{-i \mathbf{k}_{\text{in}} \cdot \mathbf{r} + i \phi_{\text{in}}(\mathbf{k}_{\text{in}})} S(\mathbf{k}_{\text{out}}, \mathbf{k}_{\text{in}}, \omega) \right|^2$$

Scan \mathbf{r} digitally \Rightarrow noninvasive image of the scattering amplitude



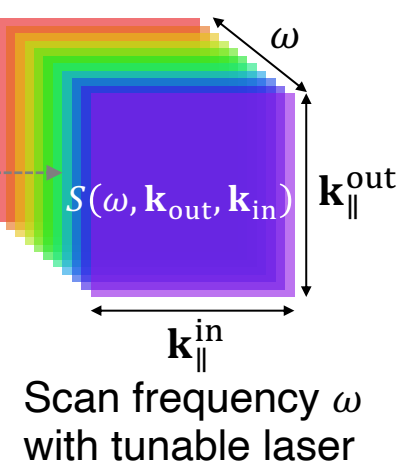
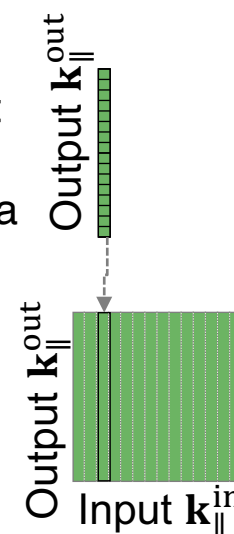
Hyper-spectral reflection matrix measurement



~ 200 frequencies ω (720-950 nm)
 ~ 4000 output angles \mathbf{k}_{out}
 ~ 3000 input angles \mathbf{k}_{in}

Map output angle $\mathbf{k}_{\parallel}^{\text{out}}$ with camera

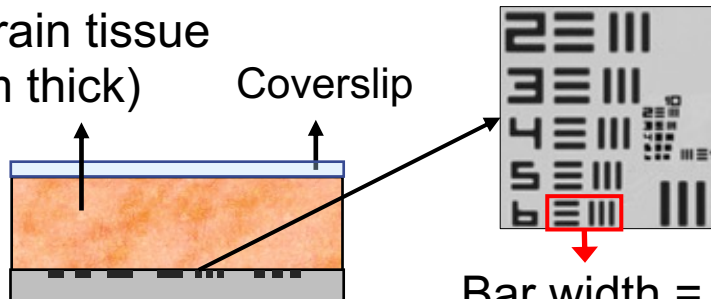
Scan input angle $\mathbf{k}_{\parallel}^{\text{in}}$ with galvo



$$I_{\text{SMT}}(\mathbf{r}) = \left| \sum_{\omega} e^{i \theta(\omega)} \sum_{\mathbf{k}_{\text{out}}} e^{i \mathbf{k}_{\text{out}} \cdot \mathbf{r} + i \phi_{\text{out}}(\mathbf{k}_{\text{out}})} \sum_{\mathbf{k}_{\text{in}}} e^{-i \mathbf{k}_{\text{in}} \cdot \mathbf{r} + i \phi_{\text{in}}(\mathbf{k}_{\text{in}})} S(\mathbf{k}_{\text{out}}, \mathbf{k}_{\text{in}}, \omega) \right|^2$$

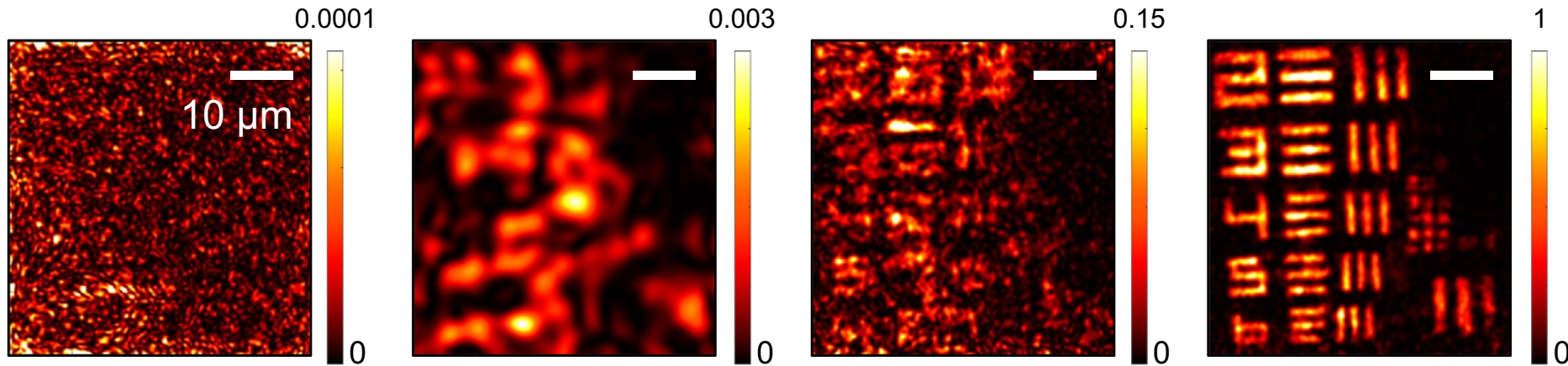
Imaging through brain tissue

Mouse brain tissue
(1 mm thick)
Coverslip
 $\lambda = 720\text{-}950 \text{ nm}$
NA = 0.5



USAF target
group 8

Bar width = 1.1 μm



Reflectance confocal
microscopy (**RCM**)

Optical coherence
tomography (**OCT**)

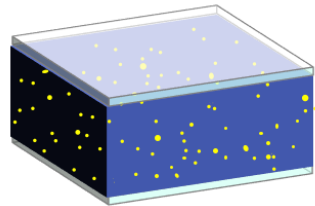
Optical coherence
microscopy (**OCM**)

SMT

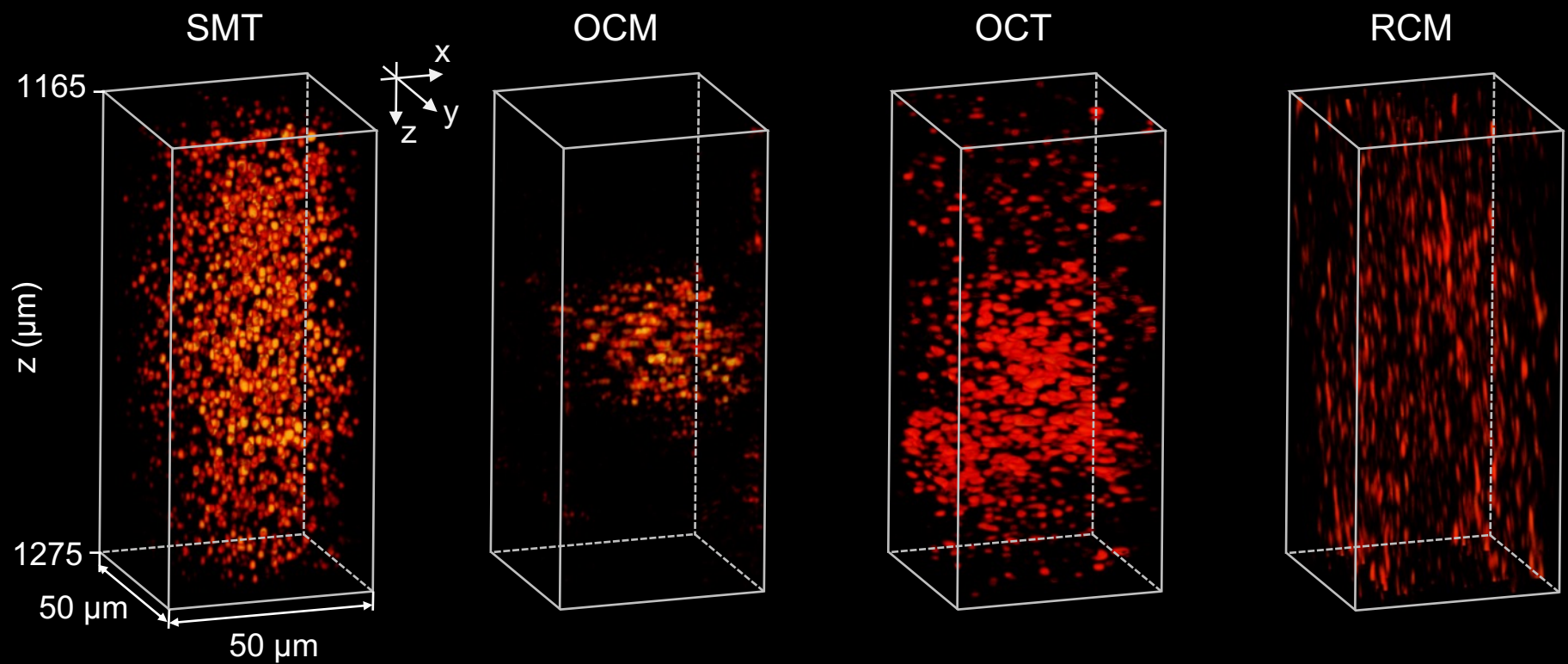
Correct for dispersion (system + sample) and
input aberration of the optical system

Also corrects for index
mismatch & scattering
from the sample

Volumetric SMT imaging

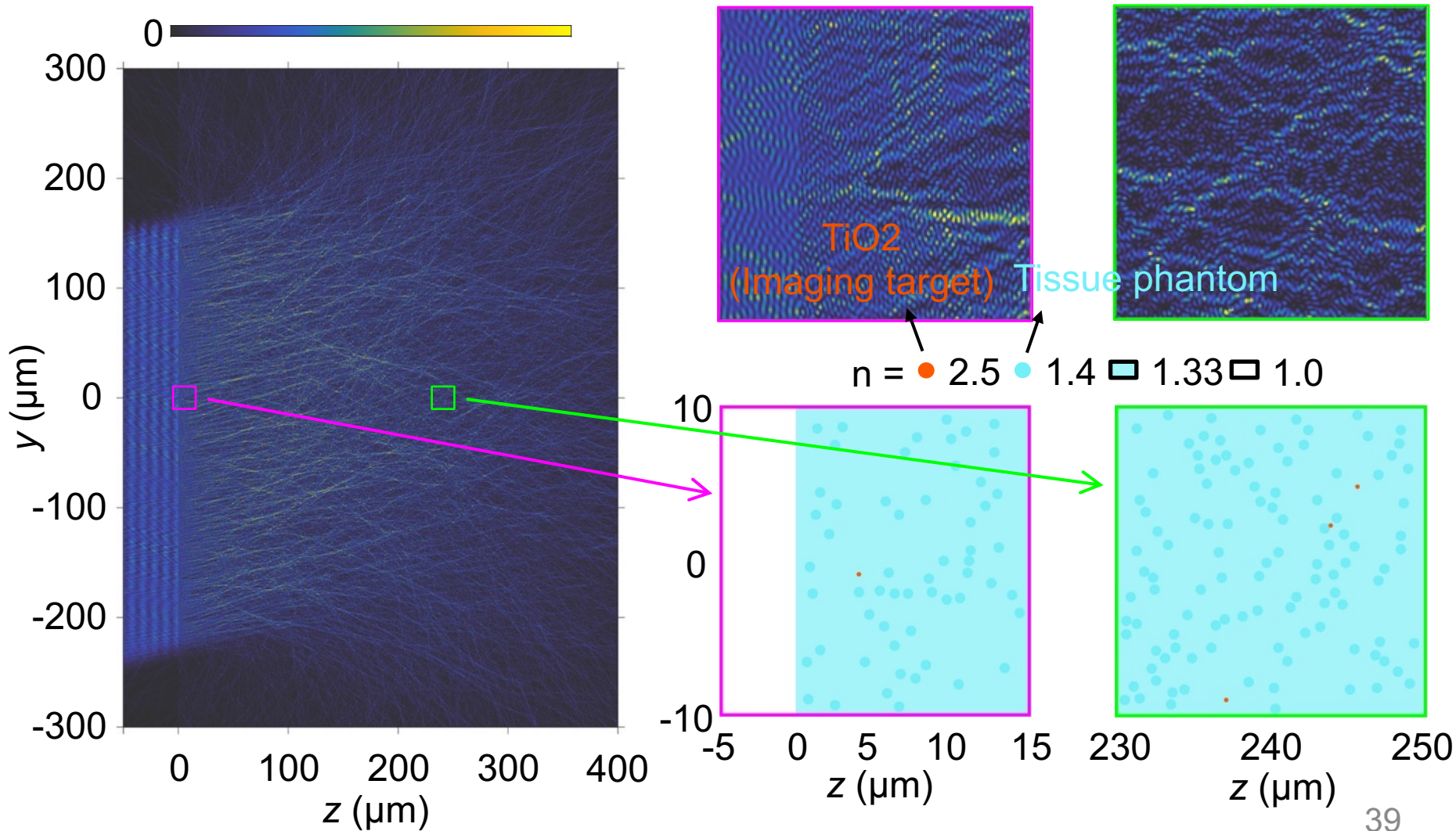


TiO_2 nanoparticles (500-nm diameter) in PDMS
Transport mean free path: 1 mm



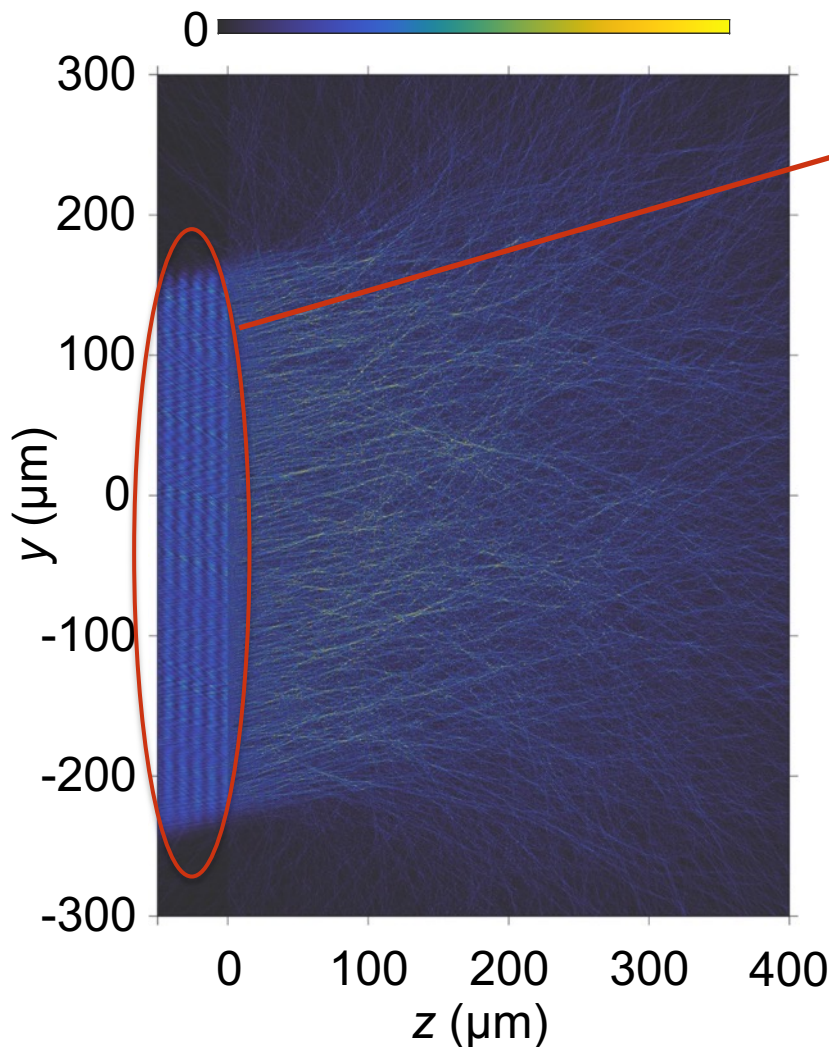
Numerical experiment with full-wave simulations

TiO_2 nanoparticles (300 nm diameter) in tissue phantom
($\ell_s = 44 \mu\text{m}$, $\ell_t = 340 \mu\text{m}$)



Numerical experiment with full-wave simulations

TiO₂ nanoparticles (300 nm diameter) in tissue phantom
($\ell_s = 44 \mu\text{m}$, $\ell_t = 340 \mu\text{m}$)



Project reflected wave onto plane waves
at different angles

⇒ One column of $R(\mathbf{k}_{\text{out}}, \mathbf{k}_{\text{in}}, \omega)$

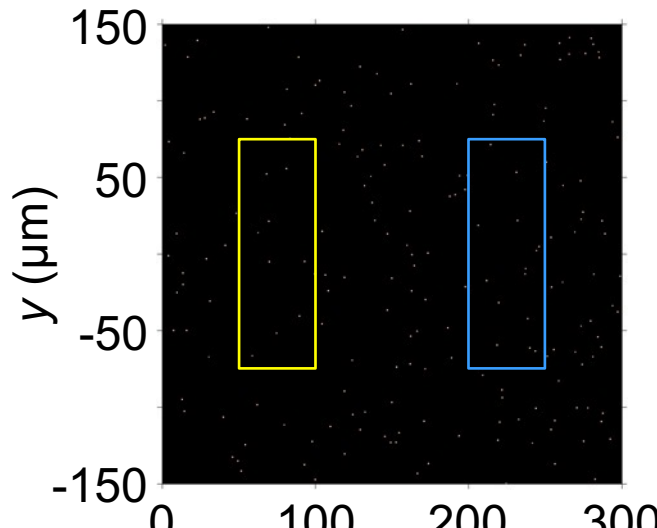
Use MESTI to compute $R(\mathbf{k}_{\text{out}}, \mathbf{k}_{\text{in}}, \omega)$
(simulation time: 4 minutes per wavelength)

Compute $R(\mathbf{k}_{\text{out}}, \mathbf{k}_{\text{in}}, \omega)$ with

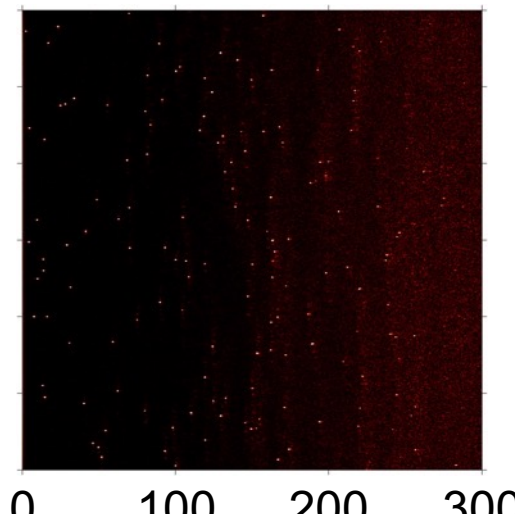
- 600 wavelengths within $\lambda \in [700, 1000] \text{ nm}$
- $\text{NA}_{\text{out}} = \text{NA}_{\text{in}} = 0.5$ (**600~900 angles each**)

SMT from full-wave simulations

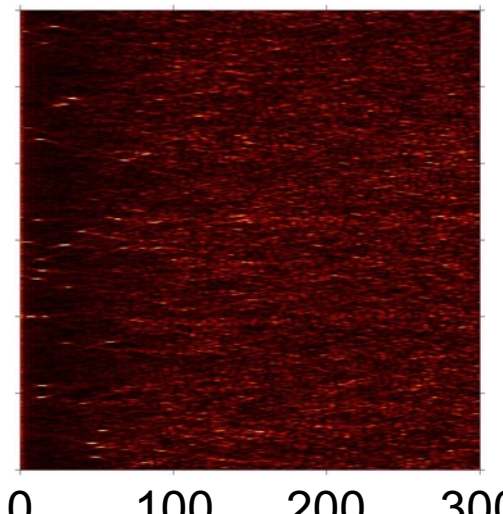
Ground truth



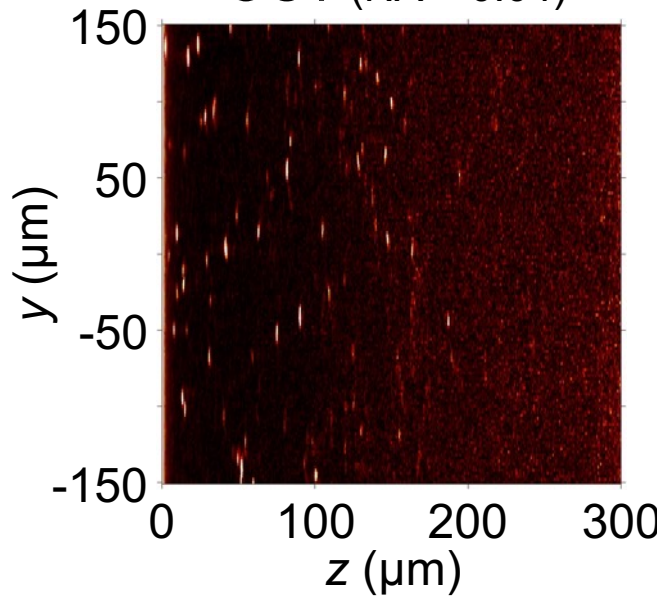
SMT



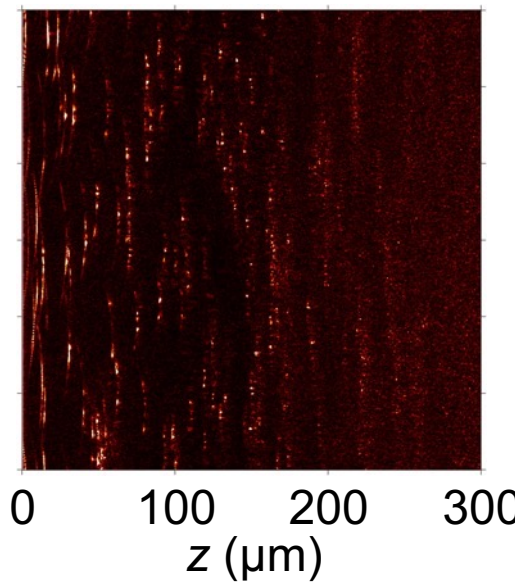
RCM



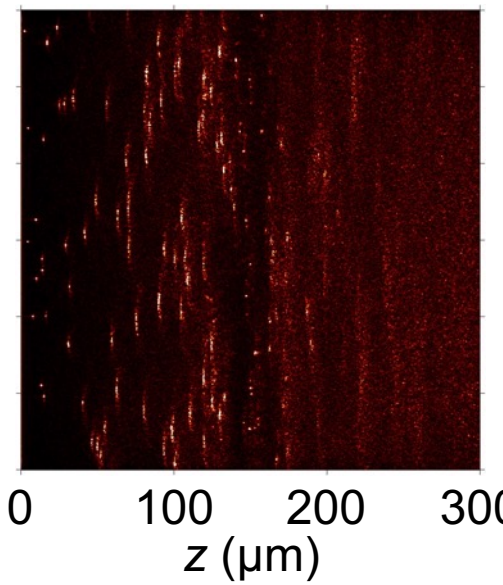
OCT (NA = 0.04)



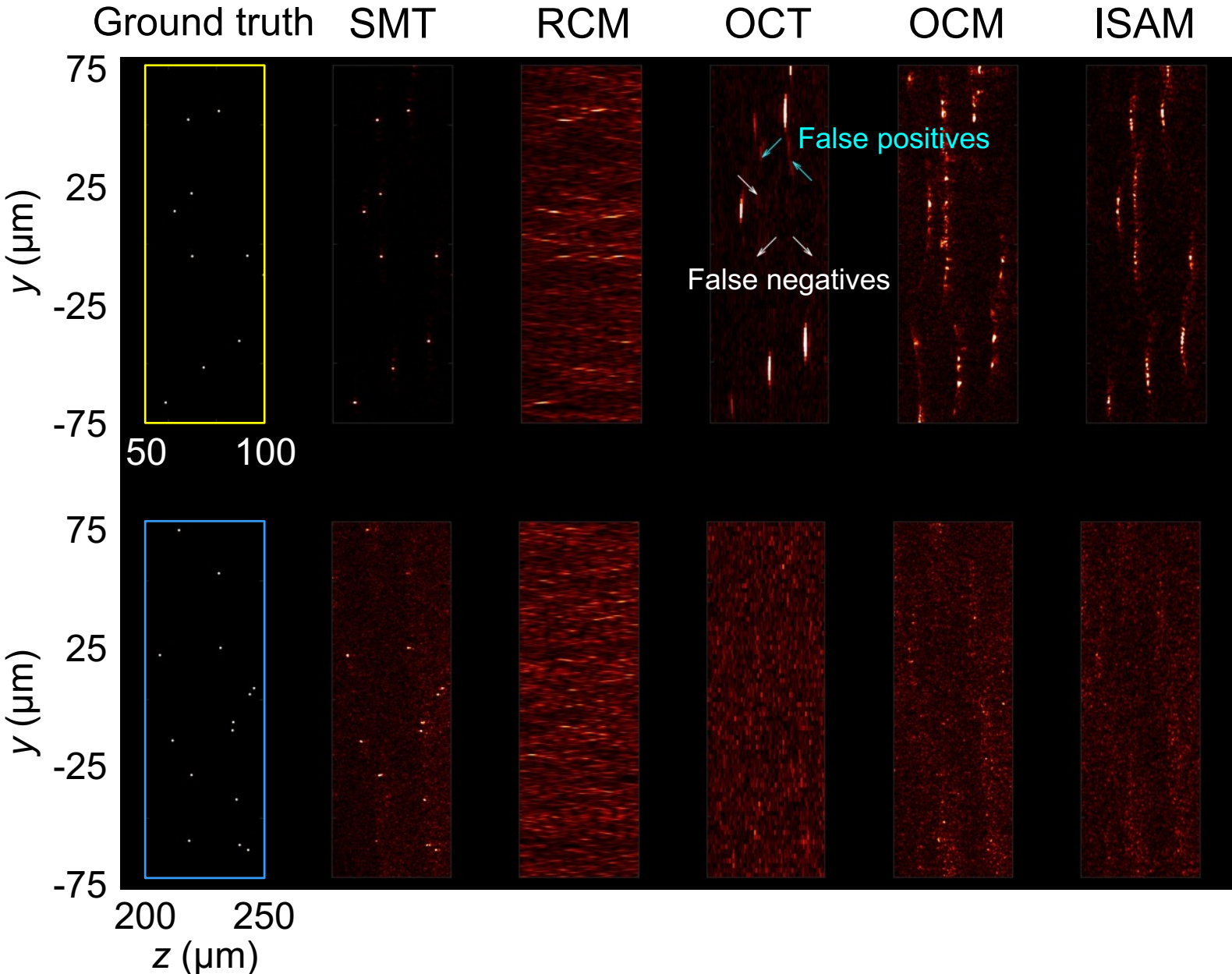
OCM (focal plane @ 150 μm)



ISAM (focal plane @ 150 μm)



Comparing methods with zoom-in

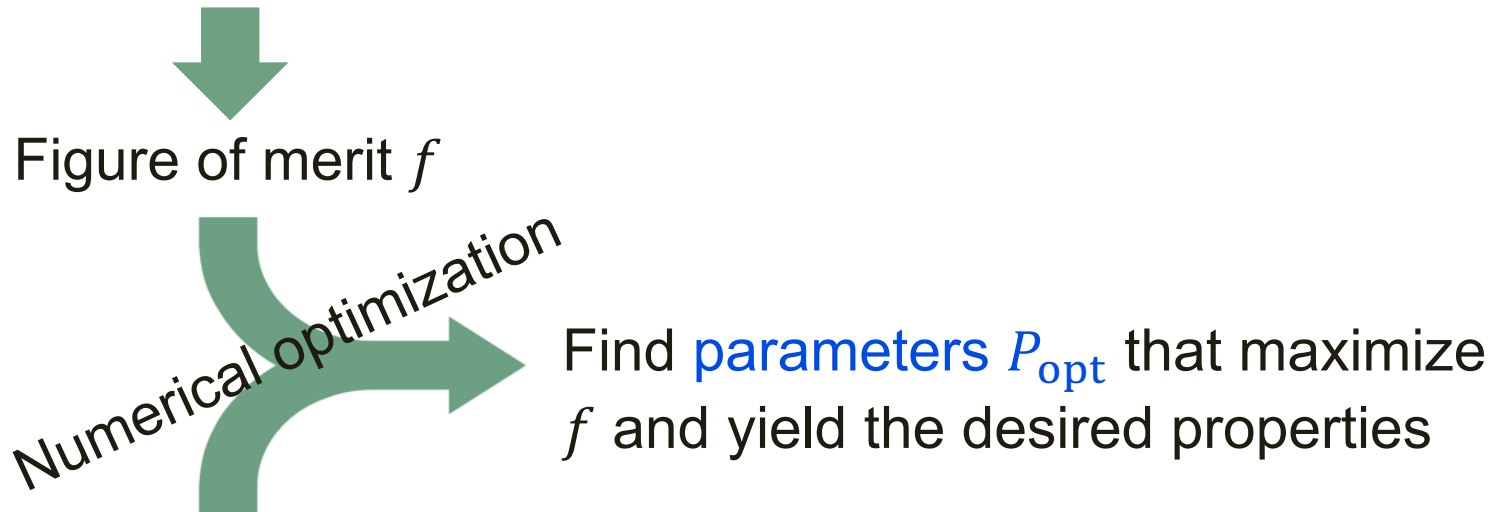


Outline

1. Augmented partial factorization (APF) method
2. Applications of APF (all done with MESTI):
 - a) Two-photon coherent backscattering
 - b) Vectorial open channel in 3D
 - c) Noninvasive imaging deep inside scattering media
 - d) **Inverse design of metasurfaces**

Inverse design

Desired properties & constraints



System parameters $P = \{p_1, \dots, p_K\}$

Efficient optimization requires the **gradient** $\vec{\nabla}_P f = \left\{ \frac{\partial f}{\partial p_1}, \dots, \frac{\partial f}{\partial p_K} \right\}$

Adjoint method:

1 input: 1 forward simulation + 1 adjoint simulation $\Rightarrow \vec{\nabla}_P f$

M inputs: M forward simulation + M adjoint simulation $\Rightarrow \vec{\nabla}_P f$

Gradient computation using APF

Figure of Merit (FoM): $f[\mathbf{S}(P), P]$

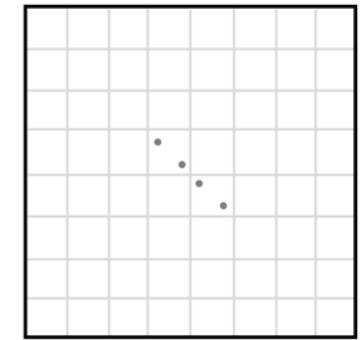
\mathbf{S} --- scattering matrix

$$\mathbf{S} = \mathbf{C}\mathbf{A}^{-1}\mathbf{B} - \mathbf{D}$$

P --- parameters to be optimized

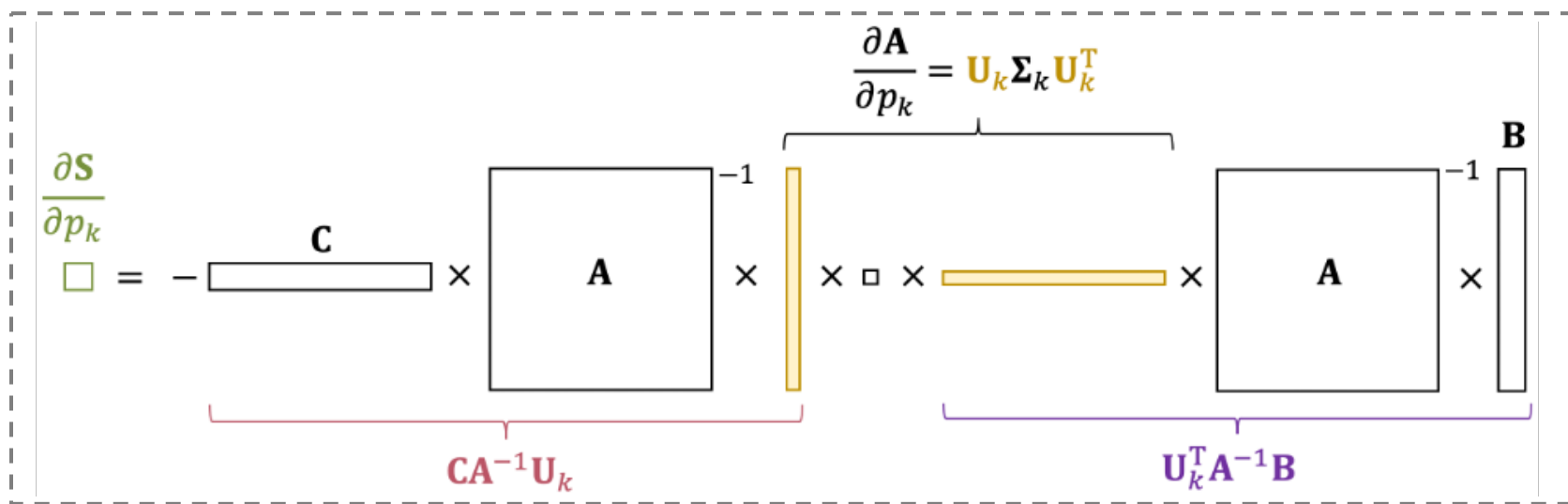
$$\frac{df}{dp_k} = \frac{\partial f}{\partial p_k} + \sum_{n,m} 2\text{Re} \left(\frac{\partial f}{\partial S_{nm}} \frac{\partial S_{nm}}{\partial p_k} \right)$$

Low-rank matrix $\partial \mathbf{A}/\partial p_k$



For a single parameter p_k :

$$\begin{aligned} \frac{\partial \mathbf{S}}{\partial p_k} &= \mathbf{C} \frac{\partial \mathbf{A}^{-1}}{\partial p_k} \mathbf{B} \\ &= -\mathbf{C}\mathbf{A}^{-1} \frac{\partial \mathbf{A}}{\partial p_k} \mathbf{A}^{-1}\mathbf{B} \\ &= -\mathbf{C}\mathbf{A}^{-1} \mathbf{U}_k \boldsymbol{\Sigma}_k \mathbf{U}_k^T \mathbf{A}^{-1}\mathbf{B} \end{aligned}$$



Gradient computation using APF

Figure of Merit (FoM): $f[\mathbf{S}(P), P]$

\mathbf{S} --- scattering matrix

$$\mathbf{S} = \mathbf{C}\mathbf{A}^{-1}\mathbf{B} - \mathbf{D}$$

P --- parameters to be optimized

$$\frac{df}{dp_k} = \frac{\partial f}{\partial p_k} + \sum_{n,m} 2\text{Re} \left(\frac{\partial f}{\partial S_{nm}} \frac{\partial S_{nm}}{\partial p_k} \right)$$

For a single parameter p_k : $\frac{\partial \mathbf{S}}{\partial p_k} = -\boxed{\mathbf{C}\mathbf{A}^{-1}\mathbf{U}_k} \Sigma_k \boxed{\mathbf{U}_k^T \mathbf{A}^{-1}\mathbf{B}}$

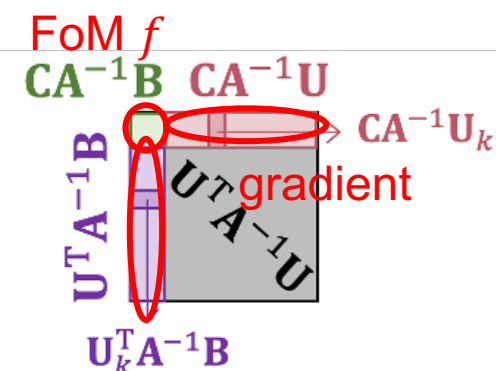
For all parameters $\{p_k\}$:

$$\begin{bmatrix} \mathbf{C} \\ \vdots \\ \mathbf{U}_k^T \end{bmatrix} \times \begin{bmatrix} \mathbf{A}^{-1} \end{bmatrix} \times \begin{bmatrix} \mathbf{B} & \cdots & \cdots \\ \mathbf{U}_k \end{bmatrix}$$

$$\mathbf{A}^{-1}$$

$$\begin{bmatrix} \mathbf{B} & \cdots & \cdots \\ \mathbf{U}_k \end{bmatrix}$$

APF



A single APF computation yields the multi-channel FoM and its gradient

Redundancy in APF... and a partial remedy

Compute using APF

$$\begin{bmatrix} \mathbf{C} \\ \mathbf{U}^T \end{bmatrix} \mathbf{A}^{-1} [\mathbf{B} \quad \mathbf{U}] \quad \Rightarrow$$

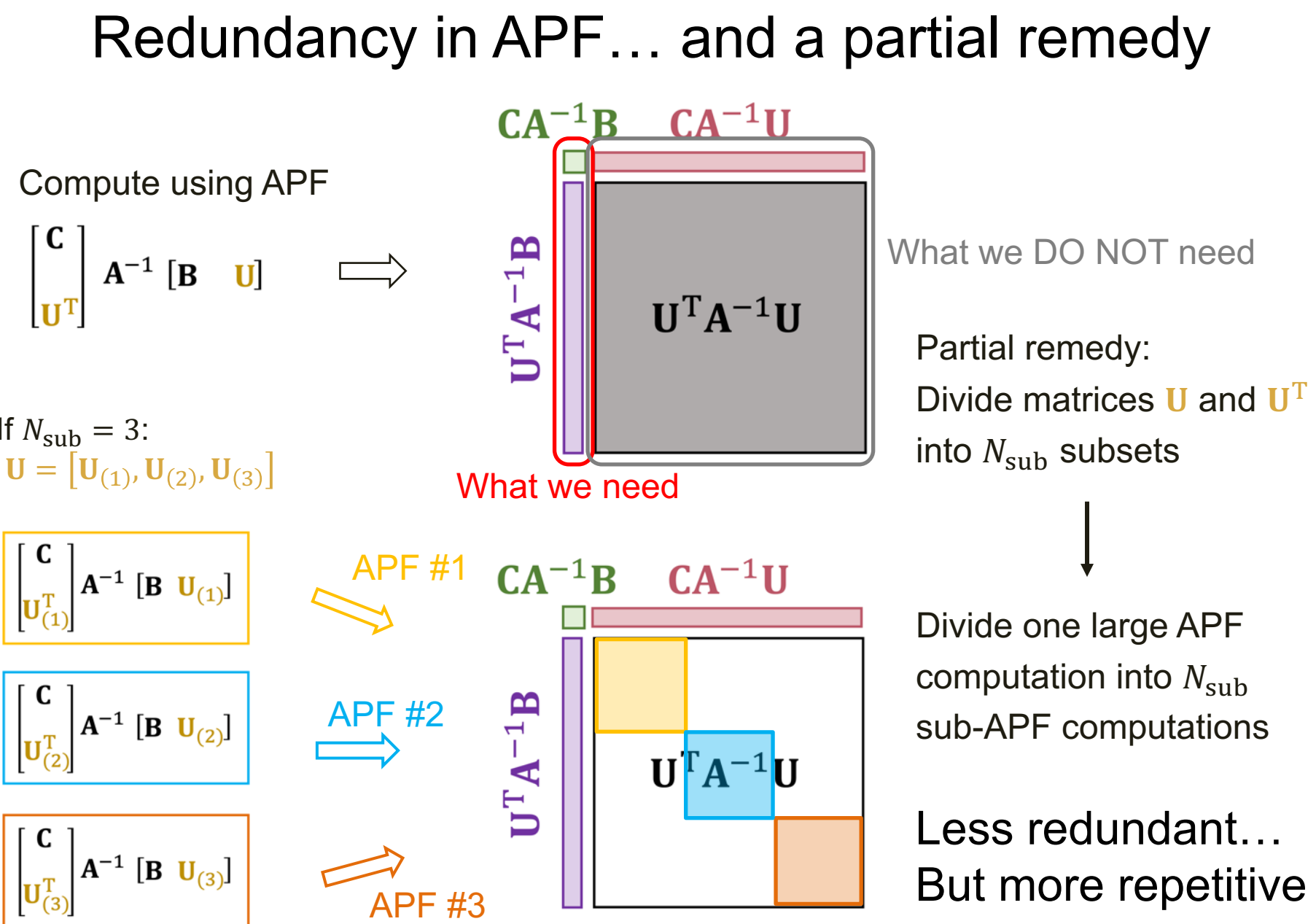
If $N_{\text{sub}} = 3$:

$$\mathbf{U} = [\mathbf{U}_{(1)}, \mathbf{U}_{(2)}, \mathbf{U}_{(3)}]$$

$$\boxed{\begin{bmatrix} \mathbf{C} \\ \mathbf{U}_{(1)}^T \end{bmatrix} \mathbf{A}^{-1} [\mathbf{B} \quad \mathbf{U}_{(1)}]}$$

$$\boxed{\begin{bmatrix} \mathbf{C} \\ \mathbf{U}_{(2)}^T \end{bmatrix} \mathbf{A}^{-1} [\mathbf{B} \quad \mathbf{U}_{(2)}]}$$

$$\boxed{\begin{bmatrix} \mathbf{C} \\ \mathbf{U}_{(3)}^T \end{bmatrix} \mathbf{A}^{-1} [\mathbf{B} \quad \mathbf{U}_{(3)}]}$$

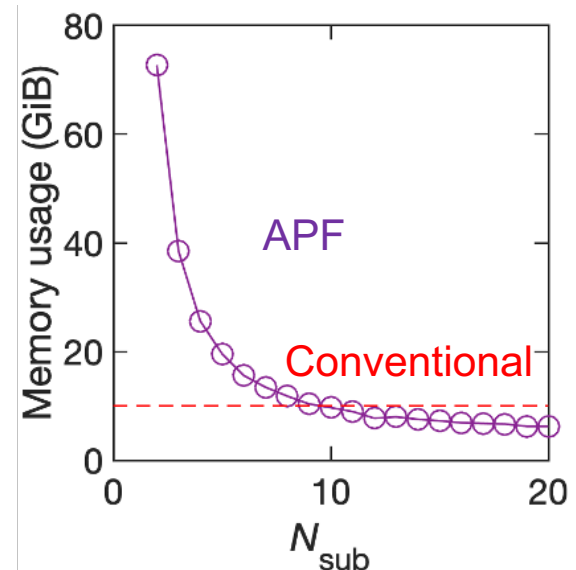
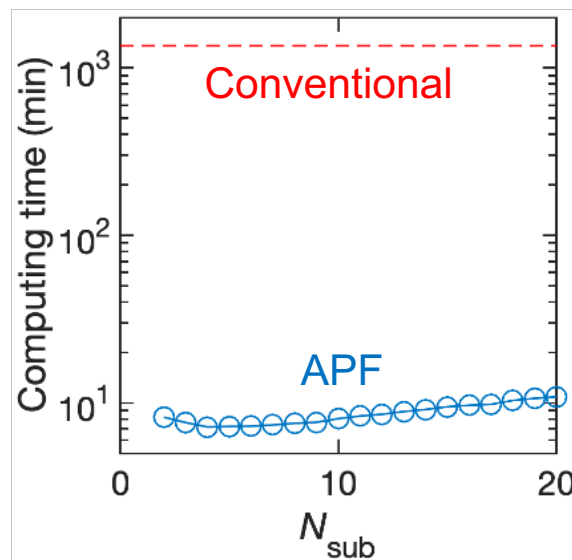
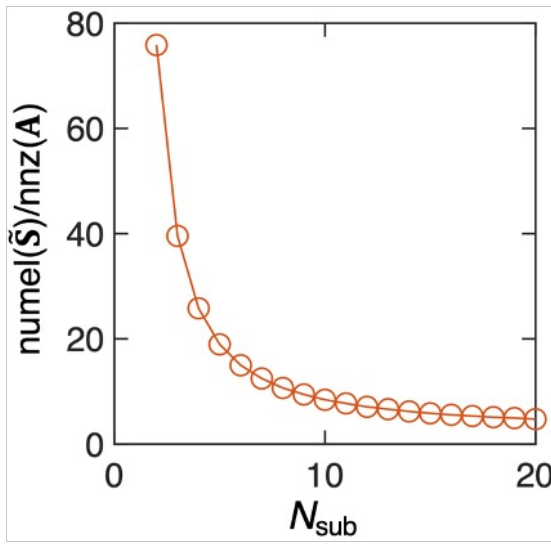


Dependence on N_{sub}

Divide one large APF computation into N_{sub} sub-APF computations

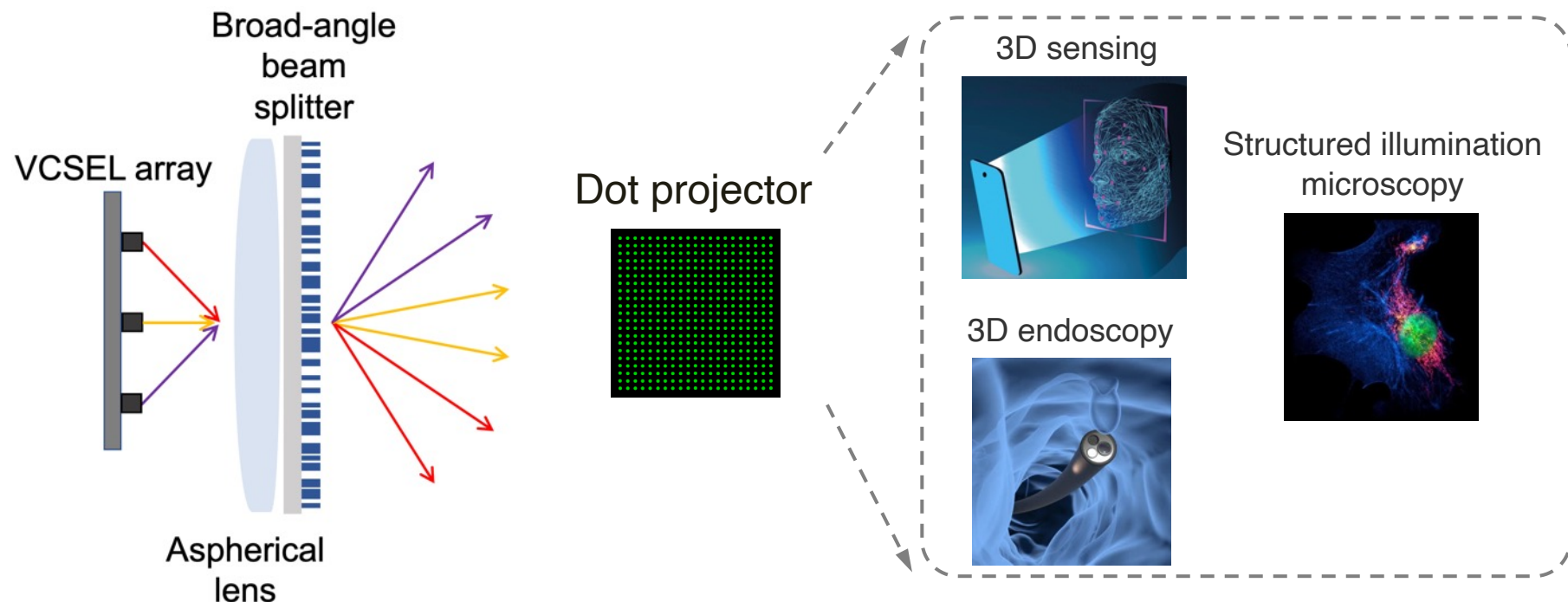
$$\tilde{\mathbf{S}} = \begin{bmatrix} \mathbf{C}\mathbf{A}^{-1}\mathbf{B} & \mathbf{C}\mathbf{A}^{-1}\mathbf{U}_{(n)} \\ \mathbf{U}_{(n)}^T\mathbf{A}^{-1}\mathbf{B} & \mathbf{U}_{(n)}^T\mathbf{A}^{-1}\mathbf{U}_{(n)} \end{bmatrix}$$

Metasurface with 1200 ridges:



Conventional adjoint method: $2M_{\text{in}}$ simulations (M_{in} forward, M_{in} adjoint)

Optimize a broad-angle metasurface beam splitter

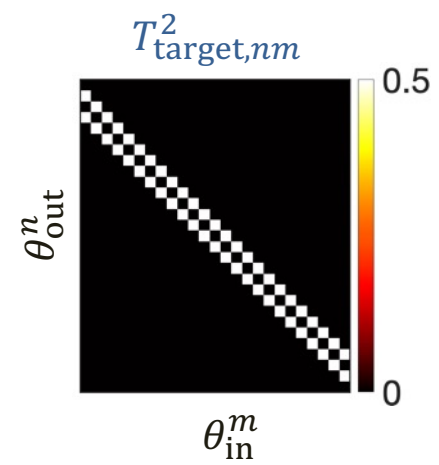


(VCSEL: Vertical-Cavity Surface-Emitting Laser)

Figure of Merit (FOM):

$$f(\mathbf{T}, P) = \sum_{n=1}^{M_{\text{out}}} \sum_{m=1}^{M_{\text{in}}} \left| |T_{nm}(P)|^2 - T_{\text{target},nm}^2 \right|^2$$

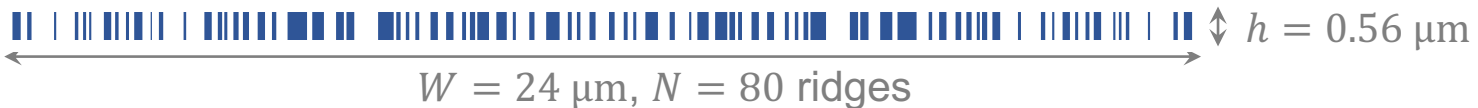
Transmission matrix: $\mathbf{T} = T_{nm} = T(\theta_{\text{out}}^n, \theta_{\text{in}}^m)$



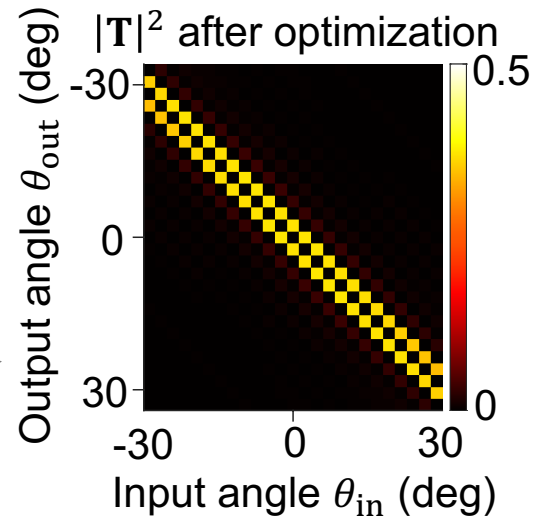
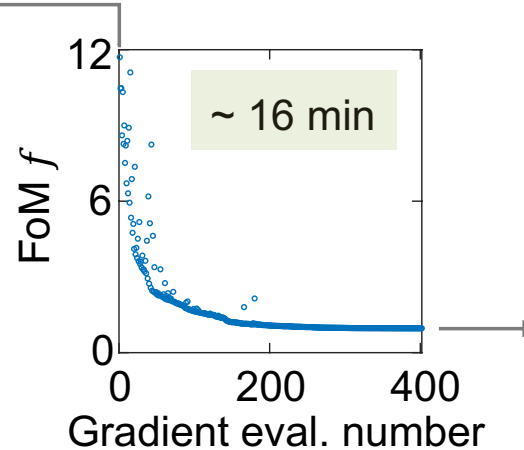
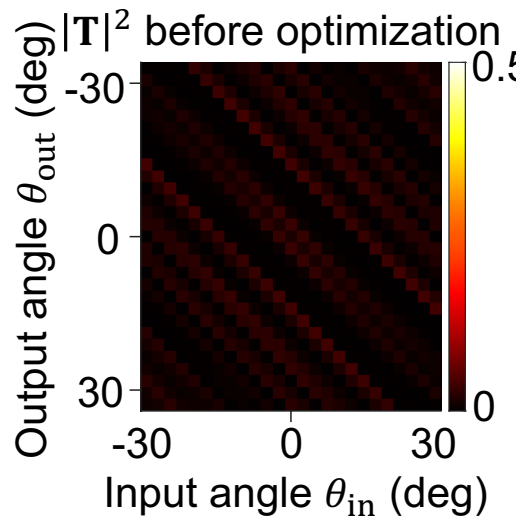
Optimize a broad-angle metasurface beam splitter

- α -Si ridges sitting on a silica-substrate. Wavelength = 940 nm
- Parameters P = {edge positions}
- Angular range = 60° , 25 input angles, 51 output angles
- Optimized with the SLSQP algorithm in NLOpt package
- Best result over 1000 randomly generated initial guesses

Before optimization:



After optimization:



Summary

1. Augmented partial factorization (APF) method
 - *Bypass unnecessary computation & Avoid repetition*
⇒ Fast computation of $\mathbf{C} \mathbf{A}^{-1} \mathbf{B}$
 - Enabled by the Schur complement feature of MUMPS
2. Applications of APF (all done with MESTI):
 - a) Two-photon coherent backscattering
 - b) Vectorial open channel in 3D
 - c) Noninvasive imaging deep inside scattering media
 - d) Inverse design of metasurfaces

Augmented partial factorization (APF) solver:

Ho-Chun Lin



Two-photon coherent backscattering:

Hebrew Univ: Mamoon Safadi, Ohad Lib,
Yaron Bromberg

Institut Langevin: Arthur Goetschy

USC: Ho-Chun Lin

Vectorial open channel in 3D:

Ho-Chun Lin

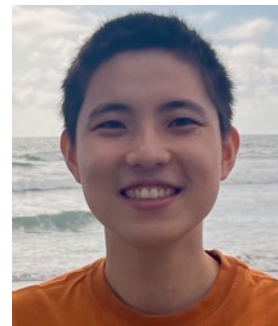
Metasurfaces inverse design:

Shiyu Li



Imaging inside scattering media:

Yiwen Zhang, Zeyu Wang, Minh Dinh



Thank you, MUMPS developers!